



HAL
open science

Guaranteed and fully robust a posteriori error estimates for conforming discretizations of diffusion problems with discontinuous coefficients

Martin Vohralík

► **To cite this version:**

Martin Vohralík. Guaranteed and fully robust a posteriori error estimates for conforming discretizations of diffusion problems with discontinuous coefficients. 2009. hal-00235810v2

HAL Id: hal-00235810

<https://hal.science/hal-00235810v2>

Preprint submitted on 25 Apr 2009 (v2), last revised 21 Jul 2010 (v4)

HAL is a multi-disciplinary open access archive for the deposit and dissemination of scientific research documents, whether they are published or not. The documents may come from teaching and research institutions in France or abroad, or from public or private research centers.

L'archive ouverte pluridisciplinaire **HAL**, est destinée au dépôt et à la diffusion de documents scientifiques de niveau recherche, publiés ou non, émanant des établissements d'enseignement et de recherche français ou étrangers, des laboratoires publics ou privés.

GUARANTEED AND FULLY ROBUST A POSTERIORI ERROR ESTIMATES FOR CONFORMING DISCRETIZATIONS OF DIFFUSION PROBLEMS WITH DISCONTINUOUS COEFFICIENTS

MARTIN VOHRALÍK

ABSTRACT. We study in this paper a posteriori error estimates for H^1 -conforming numerical approximations of diffusion problems with a scalar, piecewise constant, and arbitrarily discontinuous diffusion coefficient. We derive estimators for the energy norm and a certain dual norm which give a guaranteed global upper bound in the sense that they feature no undetermined constants. (Local) lower bounds, up to constants independent of the diffusion coefficient, are also derived. In particular, no condition on the diffusion coefficient like its monotonous increasing along paths around mesh vertices is imposed, whence the present results are fully robust and include also the cases with singular solutions. For the energy error setting, the key requirement turns out to be that the diffusion coefficient is piecewise constant on dual cells associated with the vertices of an original simplicial mesh and that harmonic averaging is used in the scheme. This is the usual case, e.g., for the cell-centered finite volume method, included in our analysis as well as the vertex-centered finite volume, finite difference, and continuous piecewise linear finite element ones. For the dual norm setting, no such a requirement is necessary. Our estimates are based on $\mathbf{H}(\text{div})$ -conforming flux reconstruction obtained thanks to the local conservativity of all the studied methods on the dual grids, which we recall in the paper, together with their mutual relations. Numerical experiments confirm the guaranteed upper bound, full robustness, and excellent efficiency of the derived estimators.

1. INTRODUCTION

We consider in this paper a model diffusion problem

$$(1.1a) \quad -\nabla \cdot (a \nabla p) = f \quad \text{in } \Omega,$$

$$(1.1b) \quad p = 0 \quad \text{on } \partial\Omega,$$

where $\Omega \subset \mathbb{R}^d$, $d = 2, 3$, is a polygonal (polyhedral) domain (open, bounded, and connected set), a is a scalar diffusion coefficient, and f is a source term. We shall derive here a posteriori error estimates for continuous piecewise linear finite element, vertex-centered finite volume, cell-centered finite volume, and finite difference approximations of this problem.

2000 *Mathematics Subject Classification*. Primary 65N15, 65N30, 76S05. Key words: finite volume method, finite element method, finite difference method, discontinuous coefficients, harmonic averaging, a posteriori error estimates, guaranteed upper bound, robustness.

This work was supported by the GNR MoMaS project “Numerical Simulations and Mathematical Modeling of Underground Nuclear Waste Disposal”, PACEN/CNRS, ANDRA, BRGM, CEA, EdF, IRSN, France.

A posteriori error estimates for finite element discretization of (1.1a)–(1.1b) have been a popular research subject starting from the Babuška and Rheinboldt work [5]. One may formulate the following five properties describing an optimal energy norm a posteriori error estimate: 1) deliver an upper bound on the error in the numerical solution which only uses the approximate solution and which can be fully, without the presence of any unknown quantities, evaluated (*guaranteed upper bound*); 2) give an expression for the estimated error locally, for example in each element of the computational mesh, and ensure that this estimate on the error represents a lower bound for the actual error, up to a generic constant (*local efficiency*); 3) ensure that the ratio of the estimated and actual error goes to one as the computational effort goes to infinity (*asymptotic exactness*); 4) guarantee the three previous properties independently of the parameters and of their variation (*robustness*); 5) give estimators which can be evaluated locally (*negligible evaluation cost*). Property 1) allows to give a certified error upper bound, 2) is crucial for the suitability of the estimates for adaptive mesh refinement, 3) and 4) ensure the optimality of the upper bound, and 5) guarantees that the evaluation cost will be much smaller than the cost required to obtain the approximate solution itself.

A vast amount of books and papers have been dedicated to the subject, cf. [3, 38] and [24, 46, 31, 17, 35, 26, 37, 21, 45, 22, 10] and the references therein. However, to the best of the author’s knowledge, none of these estimators enables to fulfill the five above properties simultaneously. The motivation of this paper was to propose estimates as close as possible to the optimality in the above sense.

One particular issue is the robustness with respect to discontinuous coefficient a . To the best of the author’s knowledge, robust estimators are only known under the ‘monotonicity around vertices’ condition on the distribution of the diffusion coefficient, see Bernardi and Verfürth [9, Hypothesis 2.7], Petzoldt [28], Ainsworth [1], or Chen and Dai [16]. The above condition is however very restrictive and in particular excludes the physically interesting cases where regions with different diffusion coefficients meet in a checkerboard pattern and where the weak solution can present singularities. We present two types of estimates which are fully robust, and this without the ‘monotonicity’ condition. The first one applies when harmonic averaging has been used in the scheme definition, and this while aligning the discontinuities of the diffusion coefficient a with a dual mesh formed around vertices. Although unusual in the finite element method, this is very common in the cell-centered finite volume (finite difference) approach. The second one applies to all the methods studied in the paper and is based on the introduction of a (nonlocal) dual norm. Estimates in this norm are then only globally efficient.

We start the paper with some preliminaries in Section 2. We then recall some useful relations between the considered methods in Section 3, so that to be able to treat them simultaneously. We next in Section 4 sketch an optimal abstract framework for a posteriori error estimation, both in the energy and dual norms. In Section 5, we then prove our a posteriori error estimates. For this purpose, we shall postprocess the original diffusive flux $-a\nabla p_h$, where p_h is the approximate solution, into $\mathbf{t}_h \in \mathbf{H}(\text{div}, \Omega)$ defined in the lowest-order Raviart–Thomas–Nédélec space on a fine simplicial mesh. Ideas in this direction have already been proposed in the literature, cf. [24, 31, 17, 26, 37, 22, 10] and go back to the Prager–Synge equality [29] and the hypercircle method [36]. We discuss four different ways of defining the equilibrated flux \mathbf{t}_h : by direct prescription, by local minimization involving

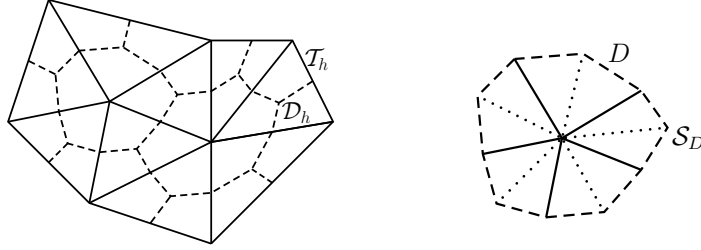


FIGURE 1. Original simplicial mesh \mathcal{T}_h and the associated dual mesh \mathcal{D}_h (left) and the fine simplicial mesh \mathcal{S}_D of $D \in \mathcal{D}_h$ (right)

local linear systems solution, by local minimization without local linear systems solution, and by mixed finite element approximations of local Neumann/Dirichlet problems. Section 5 is then closed by comparisons of the present technique with the residual, equilibrated residual, averaging, functional, and different equilibrated fluxes estimates. The proofs of the (local) efficiency and robustness are the issue of Section 6. Finally, numerical experiments are presented in Section 7.

Our results are based purely on the conservativity of all the studied methods on a dual grid and not on the Galerkin orthogonality, which is the usual case for the finite element method. The homogeneous Dirichlet boundary condition is considered only for the sake of clarity of exposition; general boundary conditions can easily be taken in account, as we outline it in [44]. This paper is a detailed description of the results previously announced in [42]; some additional numerical experiments for the finite element method, together with another local minimization strategy, are then studied in [14], and extensions to the reaction–diffusion case in [15].

2. PRELIMINARIES

We give in this section the notation and assumptions, recall some important inequalities, and finally give details on the continuous problem (1.1a)–(1.1b).

2.1. Meshes and notation. We shall work in this paper with triangulations \mathcal{T}_h which for all $h > 0$ consist of closed simplices such that $\bar{\Omega} = \bigcup_{K \in \mathcal{T}_h} K$ and which are conforming (matching), i.e., such that if $K, L \in \mathcal{T}_h$, $K \neq L$, then $K \cap L$ is either an empty set or a common face, edge, or vertex of K and L . Let h_K denote the diameter of K and let $h := \max_{K \in \mathcal{T}_h} h_K$. We denote by \mathcal{E}_h the set of all sides of \mathcal{T}_h , by $\mathcal{E}_h^{\text{int}}$ the set of interior, by $\mathcal{E}_h^{\text{ext}}$ the set of exterior, and by \mathcal{E}_K the set of all the sides of an element $K \in \mathcal{T}_h$; h_σ stands for the diameter of $\sigma \in \mathcal{E}_h$. We finally denote by \mathcal{V}_h ($\mathcal{V}_h^{\text{int}}$) the set of all (interior) vertices of \mathcal{T}_h and put, for $V \in \mathcal{V}_h$ and $K \in \mathcal{T}_h$, respectively, $\mathcal{T}_V := \{L \in \mathcal{T}_h; L \cap V \neq \emptyset\}$ and $\mathcal{T}_K := \{L \in \mathcal{T}_h; L \cap K \neq \emptyset\}$.

We shall also consider dual partitions \mathcal{D}_h of Ω such that $\bar{\Omega} = \bigcup_{D \in \mathcal{D}_h} D$ and such that for each $V \in \mathcal{V}_h$, $V \in D_V$ for exactly one $D_V \in \mathcal{D}_h$. The notation V_D stands inversely for the vertex associated with a given $D \in \mathcal{D}_h$ and we use $\mathcal{D}_h^{\text{int}}$, $\mathcal{D}_h^{\text{ext}}$ to denote the dual volumes associated with vertices from $\mathcal{V}_h^{\text{int}}$, $\mathcal{V}_h^{\text{ext}}$, respectively. Next, \mathcal{F}_h stands for all sides of \mathcal{D}_h and $\mathcal{F}_h^{\text{int}}$ ($\mathcal{F}_h^{\text{ext}}$) for all interior (exterior) sides of \mathcal{D}_h . We shall always suppose that D_V lies in the interior of the polygon/polyhedron given by \mathcal{T}_V for all $V \in \mathcal{V}_h$ and that $\mathcal{E}_h^{\text{int}} \cap \mathcal{F}_h^{\text{int}}$ has a zero ($d - 1$)-dimensional Lebesgue measure. An example of such a partition is given in the left part of Figure 1; more details on different \mathcal{D}_h considered will be given in Section 3.

In order to define our a posteriori error estimates, we will need a second conforming simplicial triangulation \mathcal{S}_h of Ω . The basic requirement is that the interiors of the elements of \mathcal{S}_h do not intersect sides of \mathcal{T}_h and \mathcal{D}_h (\mathcal{S}_h is a conforming refinement of both \mathcal{T}_h and \mathcal{D}_h). For the local efficiency proofs of our estimators, we will later need the assumption that $\{\mathcal{S}_h\}_h$ are shape-regular in the sense that there exists a constant $\kappa_{\mathcal{S}} > 0$ such that $\min_{K \in \mathcal{S}_h} |K|/h_K^d \geq \kappa_{\mathcal{S}}$ for all $h > 0$. One can easily construct a local triangulation \mathcal{S}_D of each $D \in \mathcal{D}_h$ as shown in the right part of Figure 1 and then put $\mathcal{S}_h := \cup_{D \in \mathcal{D}_h} \mathcal{S}_D$. We will use the notation \mathcal{G}_h for all sides of \mathcal{S}_h and $\mathcal{G}_h^{\text{int}}$ ($\mathcal{G}_h^{\text{ext}}$) for all interior (exterior) sides of \mathcal{S}_h .

Next, for $K \in \mathcal{T}_h$, \mathbf{n} will always denote its exterior normal vector; we shall also employ the notation \mathbf{n}_σ for a normal vector of a side $\sigma \in \mathcal{E}_h$, whose orientation is chosen arbitrarily but fixed for interior sides and coinciding with the exterior normal of Ω for exterior sides. For $\sigma \in \mathcal{E}_h^{\text{int}}$ shared by $K, L \in \mathcal{T}_h$ (which we denote by $\sigma_{K,L}$) such that \mathbf{n}_σ points from K to L and a function φ , we shall define the jump operator $[[\cdot]]$ by

$$(2.1) \quad [[\varphi]] := (\varphi|_K)|_\sigma - (\varphi|_L)|_\sigma.$$

We put $[[\varphi]]_\sigma := \varphi|_\sigma$ for any $\sigma \in \mathcal{E}_h^{\text{ext}}$. We next associate with each $K \in \mathcal{T}_h$ and each $\sigma \in \mathcal{E}_K$ a weight $\omega_{K,\sigma}$ such that

$$(2.2a) \quad 0 \leq \omega_{K,\sigma} \leq 1 \quad \forall K \in \mathcal{T}_h, \forall \sigma \in \mathcal{E}_K,$$

$$(2.2b) \quad \omega_{K,\sigma} + \omega_{L,\sigma} = 1 \quad \forall \sigma = \sigma_{K,L} \in \mathcal{E}_h^{\text{int}},$$

$$(2.2c) \quad \omega_{K,\sigma} = 1 \quad \forall \sigma \in \mathcal{E}_h^{\text{ext}} \text{ and } K \in \mathcal{T}_h \text{ such that } \sigma \in \mathcal{E}_K.$$

For $\sigma = \sigma_{K,L} \in \mathcal{E}_h^{\text{int}}$, we define the weighted average operator $\{\!\!\{ \cdot \}\!\!\}_\omega$ by

$$(2.3) \quad \{\!\!\{ \varphi \}\!\!\}_\omega := \omega_{K,\sigma}(\varphi|_K)|_\sigma + \omega_{L,\sigma}(\varphi|_L)|_\sigma,$$

whereas for $\sigma \in \mathcal{E}_h^{\text{ext}}$, $\{\!\!\{ \varphi \}\!\!\}_\omega := \varphi|_\sigma$. We denote by $\{\!\!\{ \varphi \}\!\!\}$ the standard average operator with $\omega_{K,\sigma} = \omega_{L,\sigma} = \frac{1}{2}$ and $\{\!\!\{ \varphi \}\!\!\} := \varphi|_\sigma$ for $\sigma \in \mathcal{E}_h^{\text{ext}}$. We use the same type of notation also for the meshes \mathcal{D}_h and \mathcal{S}_h .

We shall be working below with numerical methods whose approximate solution can be represented by continuous piecewise linear functions on \mathcal{T}_h , with value 0 at the boundary of Ω . The basis of this space, denoted by X_h^0 , is spanned by the classical pyramidal functions ψ_V , $V \in \mathcal{V}_h^{\text{int}}$, such that $\psi_V(U) = \delta_{VU}$, $U \in \mathcal{V}_h$, δ being the Kronecker delta.

In what concerns functional notation, we denote by $(\cdot, \cdot)_S$ the L^2 -scalar product on S and by $\|\cdot\|_S$ the associated norm; when $S = \Omega$, the index is dropped off. We mean by $|S|$ the Lebesgue measure of S , by $|\sigma|$ the $(d-1)$ -dimensional Lebesgue measure of $\sigma \subset \mathbb{R}^{d-1}$, and in particular by $|\mathbf{s}|$ the length of a segment \mathbf{s} . Next, $H^1(S)$ is the Sobolev space of functions with square-integrable weak derivatives and $H_0^1(S)$ is its subspace of functions with traces vanishing on ∂S . Finally, $\mathbf{H}(\text{div}, S)$ is the space of functions with square-integrable weak divergences, $\mathbf{H}(\text{div}, S) = \{\mathbf{v} \in \mathbf{L}^2(S); \nabla \cdot \mathbf{v} \in L^2(S)\}$, and $\langle \cdot, \cdot \rangle_{\partial S}$ stands for the appropriate duality pairing on ∂S .

2.2. Assumptions. We shall suppose that $f(\mathbf{x}) \in L^2(\Omega)$ and that $a(\mathbf{x})$ is a piecewise constant scalar-valued function. We in particular consider cases where a is piecewise constant on the triangulation \mathcal{T}_h and cases where a is piecewise constant on the dual partition \mathcal{D}_h . In all cases we denote by $c_{a,K}$ and $C_{a,K}$ for all $K \in \mathcal{T}_h$ the best positive constants such that $c_{a,K} \leq a(\mathbf{x}) \leq C_{a,K}$ for all $\mathbf{x} \in K$. Similar notation will be used also for $D \in \mathcal{D}_h$, for \mathcal{T}_K , $K \in \mathcal{T}_h$, or for the entire domain.

2.3. Poincaré and Friedrichs inequalities. Let D be a polygon or a polyhedron. The Poincaré inequality states that

$$(2.4) \quad \|\varphi - \varphi_D\|_D^2 \leq C_{P,D} h_D^2 \|\nabla \varphi\|_D^2 \quad \forall \varphi \in H^1(D),$$

where φ_D is the mean of φ over D given by $\varphi_D := (\varphi, 1)_D / |D|$ and where the constant $C_{P,D}$ can for each convex D be evaluated as $1/\pi^2$, cf. [27, 8]. To evaluate $C_{P,D}$ for nonconvex elements D is more complicated but it still can be done, cf. [20, Lemma 10.2] or [12, Section 2].

Lest $|\partial\Omega \cap \partial D| \neq 0$. Then the Friedrichs inequality states that

$$(2.5) \quad \|\varphi\|_D^2 \leq C_{F,D,\partial\Omega} h_D^2 \|\nabla \varphi\|_D^2 \quad \forall \varphi \in H^1(D) \text{ such that } \varphi = 0 \text{ on } \partial\Omega \cap \partial D.$$

As long as $\partial\Omega$ is such that there exists a vector $\mathbf{b} \in \mathbb{R}^d$ such that for almost all $\mathbf{x} \in D$, the first intersection of $\mathcal{B}_{\mathbf{x}}$ and ∂D lies in $\partial\Omega$, where $\mathcal{B}_{\mathbf{x}}$ is the straight semi-line defined by the origin \mathbf{x} and the vector \mathbf{b} , $C_{F,D,\partial\Omega} = 1$, cf. [40, Remark 5.8]. To evaluate $C_{F,D,\partial\Omega}$ in the general case is more complicated but it still can be done, cf. [40, Remark 5.9] or [12, Section 3].

2.4. Continuous problem. We define a bilinear form \mathcal{B} by

$$(2.6) \quad \mathcal{B}(p, q) := (a \nabla p, \nabla q) \quad p, q \in H_0^1(\Omega).$$

The weak formulation of problem (1.1a)–(1.1b) is to find $p \in H_0^1(\Omega)$ such that

$$(2.7) \quad \mathcal{B}(p, q) = (f, q) \quad \forall q \in H_0^1(\Omega)$$

and the corresponding energy norm is defined by

$$(2.8) \quad \|q\|^2 := \mathcal{B}(q, q) = \|a^{\frac{1}{2}} \nabla q\|^2, \quad q \in H_0^1(\Omega).$$

Alternatively, following the approaches of Verfürth [39] and Chaillou and Suri [13] of the convection–diffusion and nonlinear settings, respectively, we will also present a posteriori error estimates in a dual norm. We will use

$$(2.9) \quad \|q\|_{\#} := \sup_{\varphi \in H_0^1(\Omega)} \frac{\mathcal{B}(q, \varphi)}{\|\nabla \varphi\|}, \quad q \in H_0^1(\Omega)$$

for this purpose.

Remark 2.1 (Energy and dual norms). The energy norm (2.8) admits a local decomposition and is easily computable. The dual norm (2.9) is a global norm and its practical computation is not obvious except of particular cases. In any case, however, it is immediate from (2.9) that there exist easily and locally computable upper and lower bounds for $\|\cdot\|_{\#}$:

$$(2.10) \quad \frac{\|a^{\frac{1}{2}} \nabla q\|^2}{\|\nabla q\|} \leq \|q\|_{\#} \leq \|a \nabla q\|.$$

In particular, the two above norms coincide when $a = 1$.

3. SOME H^1 -CONFORMING METHODS AND THEIR MUTUAL RELATIONS

The purpose of this section is to recall several classical numerical methods for problem (1.1a)–(1.1b) and their mutual relations. Using these relations, the a posteriori error estimates derived in this paper will apply to all these methods. This section may be skipped temporarily if the reader is only interested in the global a posteriori error upper bounds (Sections 4 and 5.1 below).

3.1. Definitions. We start by giving the definitions.

Definition 3.1 (Weighted cell-centered finite volume method). Let \mathcal{D}_h be the Voronoï grid given by the vertices from \mathcal{V}_h , cf. Eymard *et al.* [20] (this requires that the vertices $V \in \mathcal{V}_h^{\text{ext}}$ are suitably placed so that $\bar{\Omega} = \bigcup_{D \in \mathcal{D}_h} D$). Let next $\mathcal{N}(D)$ denote the set of “neighbors” of $D \in \mathcal{D}_h$, i.e., of such $E \in \mathcal{D}_h$ that $\sigma_{D,E} := \partial D \cap \partial E$ is such that $|\sigma_{D,E}| \neq 0$; in such a case, let $d_{D,E}$ stand for the Euclidean distance of the associated vertices V_D and V_E . Let finally a be piecewise constant on \mathcal{D}_h . Then the weighted cell-centered finite volume method for problem (1.1a)–(1.1b) reads: find $p_h = \sum_{D \in \mathcal{D}_h} p_D \psi_{V_D}$, with $p_D = 0$ for all $D \in \mathcal{D}_h^{\text{ext}}$ so that $p_h \in X_h^0$, such that

$$(3.1) \quad - \sum_{E \in \mathcal{N}(D)} \{a\}_\omega \frac{|\sigma_{D,E}|}{d_{D,E}} (p_E - p_D) = (f, 1)_D \quad \forall D \in \mathcal{D}_h^{\text{int}}.$$

Here, two basic choices for the weights in $\{a\}_\omega$ on a side $\sigma = \sigma_{D,E} \in \mathcal{F}_h^{\text{int}}$ exist:

$$(3.2) \quad \omega_{D,\sigma} = \omega_{E,\sigma} = \frac{1}{2},$$

which corresponds to the arithmetic averaging, and

$$(3.3) \quad \omega_{D,\sigma} = \frac{a_E}{a_D + a_E}, \quad \omega_{E,\sigma} = \frac{a_D}{a_D + a_E},$$

which corresponds to the harmonic averaging.

Definition 3.2 (Vertex-centered finite volume method). Let the dual grid \mathcal{D}_h consist of polygonal/polyhedral dual volumes and let a be piecewise constant on \mathcal{T}_h so that a is not double-valued on $\mathcal{F}_h^{\text{int}}$. Then the vertex-centered finite volume method for problem (1.1a)–(1.1b) reads: find $p_h \in X_h^0$ such that

$$(3.4) \quad - \langle a \nabla p_h \cdot \mathbf{n}, 1 \rangle_{\partial D} = (f, 1)_D \quad \forall D \in \mathcal{D}_h^{\text{int}}.$$

Definition 3.3 (Weighted vertex-centered finite volume method). Let the dual grid \mathcal{D}_h consist of polygonal/polyhedral dual volumes. Then we can design a weighted vertex-centered finite volume method for problem (1.1a)–(1.1b) as follows: find $p_h \in X_h^0$ such that

$$(3.5) \quad - \langle \{a\}_\omega \nabla p_h \cdot \mathbf{n}, 1 \rangle_{\partial D} = (f, 1)_D \quad \forall D \in \mathcal{D}_h^{\text{int}}.$$

Remark 3.4 (Arithmetic/harmonic averaging in the vertex-centered finite volume method). We first remark that when a is piecewise constant on \mathcal{T}_h , the above definition coincides with the standard Definition 3.2, which is known to lead to arithmetic-like averaging of a . When, however, a is piecewise constant on \mathcal{D}_h , then as in the cell-centered finite volume case, the two basic choices for the weights in $\{a\}_\omega$, (3.2) and (3.3), lead respectively to arithmetic and harmonic averaging of a .

Definition 3.5 (Finite element method). The finite element method for problem (1.1a)–(1.1b) reads: find $p_h \in X_h^0$ such that

$$(3.6) \quad (a \nabla p_h, \nabla \psi_V)_{\mathcal{T}_V} = (f, \psi_V)_{\mathcal{T}_V} \quad \forall V \in \mathcal{V}_h^{\text{int}}.$$

Definition 3.6 (Finite element method with harmonic averaging). Let the dual grid \mathcal{D}_h consist of polygonal/polyhedral dual volumes and let a be piecewise constant on \mathcal{D}_h . Let us define \tilde{a} by

$$(3.7) \quad \tilde{a}|_K = \left(\frac{(a^{-1}, 1)_K}{|K|} \right)^{-1} \quad \forall K \in \mathcal{T}_h.$$

Then we can define a finite element method with harmonic averaging for problem (1.1a)–(1.1b) as: find $p_h \in X_h^0$ such that

$$(3.8) \quad (\tilde{a}\nabla p_h, \nabla \psi_V)_{\mathcal{T}_V} = (f, \psi_V)_{\mathcal{T}_V} \quad \forall V \in \mathcal{V}_h^{\text{int}}.$$

Remark 3.7 (Arithmetic/harmonic averaging in the finite element method). We remark that the difference between the matrices of (3.6) and (3.8) corresponds to the difference between the matrices of the piecewise linear nonconforming finite element method and that of the hybridization of the lowest-order Raviart–Thomas mixed finite element method in that the first ones use the arithmetic and the second ones use the harmonic averaging of the diffusion coefficient a , cf. [4]. In particular, by Definitions 3.5 and 3.6, one has in the finite element method the choice between the arithmetic and the harmonic averaging as in the finite volume one.

3.2. Equivalences. We are now ready to recall several equivalence results between the above methods.

Lemma 3.8 (Equivalence between matrices of finite elements and vertex-centered finite volumes). *Let $D \in \mathcal{D}_h$ have Lipschitz-continuous boundaries and let $|\sigma \cap D| = |\sigma|/d$ for each $\sigma \in \mathcal{E}_h^{\text{int}}$ with a vertex $V_D \in \mathcal{V}_h^{\text{int}}$ and the associated $D \in \mathcal{D}_h^{\text{int}}$. Let, moreover, a be piecewise constant on \mathcal{T}_h . Then, for all $p_h \in X_h^0$,*

$$(3.9) \quad (a\nabla p_h, \nabla \psi_{V_D})_{\mathcal{T}_{V_D}} = -\langle a\nabla p_h \cdot \mathbf{n}, 1 \rangle_{\partial D} \quad \forall D \in \mathcal{D}_h^{\text{int}}.$$

Proof. Employing the Green theorem and the finite elements basis functions form, see [7, Lemma 3] for $d = 2$. \square

Lemma 3.9 (Equivalence between matrices of finite elements and cell-centered finite volumes). *Let $d = 2$, let \mathcal{T}_h be Delaunay, that is let the circumcircle of each triangle does not contain any vertex in its interior, and let, moreover, no circumcenters of boundary triangles lie outside the domain Ω . Let \mathcal{D}_h be the Voronoi grid given by the vertices from \mathcal{V}_h and let $a = 1$. Then, for all $p_h \in X_h^0$,*

$$(\nabla p_h, \nabla \psi_{V_D})_{\mathcal{T}_{V_D}} = - \sum_{E \in \mathcal{N}(D)} \frac{|\sigma_{D,E}|}{d_{D,E}} (p_E - p_D) \quad \forall D \in \mathcal{D}_h^{\text{int}}.$$

Proof. See [20, Section III.12]. \square

Remark 3.10 (Relation between finite elements and cell-centered finite volumes if $d = 3$). We remark that the above lemma does not generalize to three space dimensions, see, e.g., Letniowski [25] or Putti and Cordes [30].

Lemma 3.11 (Equivalence between right-hand sides of finite elements and finite volumes). *Let $|D \cap K| = |K|/(d+1)$ for each $D \in \mathcal{D}_h^{\text{int}}$ and each $K \in \mathcal{T}_{V_D}$. Let, moreover, f be piecewise constant on \mathcal{T}_h . Then*

$$(3.10) \quad (f, \psi_{V_D})_{\mathcal{T}_{V_D}} = (f, 1)_D \quad \forall D \in \mathcal{D}_h^{\text{int}}.$$

Proof. Straightforward using the condition $|D \cap K| = |K|/(d+1)$ for $D \in \mathcal{D}_h^{\text{int}}$ and $K \in \mathcal{T}_{V_D}$ and a quadrature formula for linear functions on simplices. \square

3.3. Consequences. The following corollaries are obvious consequences of the previous lemmas.

Corollary 3.12 (Equivalence between finite elements and vertex-centered finite volumes). *Let the assumptions of Lemmas 3.8 and 3.11 be verified. Then the finite element method given by Definition 3.5 and the vertex-centered finite volume methods given by Definitions 3.2 and 3.3 produce the same discrete systems.*

Corollary 3.13 (Local conservativity of the finite element method on dual grids). *Let the assumptions of Lemmas 3.8 and 3.11 be verified. Then the finite element method given by Definition 3.5 is locally conservative over the dual grid $\mathcal{D}_h^{\text{int}}$.*

Corollary 3.14 (Equivalence between weighted cell- and vertex-centered finite volumes). *Let $d = 2$, let \mathcal{T}_h be Delaunay, let no circumcenters of boundary triangles lie outside the domain Ω , and let \mathcal{D}_h be the Voronoï grid given by the vertices from \mathcal{V}_h . Let next a be piecewise constant on \mathcal{D}_h . Then the weighted cell-centered finite volume method given by Definition 3.1 and the weighted vertex-centered finite volume method given by Definition 3.3 produce the same discrete systems.*

3.4. Remarks. We finish this section by some additional remarks.

Remark 3.15 (Local conservativity of the finite element method). Corollary 3.13 should be understood in the following sense: First of all, equation (3.4) states that the sum of fluxes entering/leaving $D \in \mathcal{D}_h^{\text{int}}$ equals the sources on this element. Secondly, rewriting $-\langle a \nabla p_h \cdot \mathbf{n}, 1 \rangle_{\partial D}$ as $-\sum_{E \in \mathcal{N}(D)} \langle a \nabla p_h \cdot \mathbf{n}, 1 \rangle_{\sigma_{D,E}}$ and noticing that the quantity $a \nabla p_h \cdot \mathbf{n}$ is single-valued on $\sigma_{D,E}$ under the given assumptions, local mass balance, in the sense that the mass leaving from one element (D) enters its neighbor (E), is likewise satisfied. Consequently, the finite element method is well locally mass conservative on $\mathcal{D}_h^{\text{int}}$, even if it is not locally mass conservative on \mathcal{T}_h . Remark finally that the above assertions are only valid exactly if in particular a and f are piecewise constant on \mathcal{T}_h . In the general case, local mass conservativity on \mathcal{D}_h only holds up to a numerical quadrature/data oscillation.

Remark 3.16 (Choice of the dual grids). In the above developments, a large freedom is left in what concerns the actual choice of the dual grids \mathcal{D}_h . The basic and most frequently used grid satisfying both the assumptions of Lemmas 3.8 and 3.11 is given by straight lines connecting the triangle barycentres through the midpoints of the edges of \mathcal{T}_h if $d = 2$ and similarly if $d = 3$.

Remark 3.17 (Finite difference method). Let \mathcal{D}_h consist of squares if $d = 2$ and cubes if $d = 3$. Then the finite difference method for problem (1.1a)–(1.1b) coincides with cell-centered finite volume one given by Definition 3.1, cf. Eymard *et al.* [20].

Remark 3.18 (Tensor-valued diffusion coefficients). In problem (1.1a)–(1.1b), we could also consider a tensor-valued diffusion coefficient \mathbf{A} in place of the scalar-valued a . Definitions 3.5 and 3.6 would in this case contain \mathbf{A} in place of a and similarly for Definitions 3.2 and 3.3. Then, for \mathbf{A} piecewise constant on \mathcal{T}_h , Lemma 3.8 still holds true and similarly for Corollaries 3.12 and 3.13.

4. OPTIMAL ABSTRACT FRAMEWORK FOR A POSTERIORI ERROR ESTIMATION

We give here an optimal abstract framework for a posteriori error estimation in problem (1.1a)–(1.1b) in the energy norm (2.8). The basic ideas can be traced back to the Prager–Synge equality [29], the hypercircle method [36], and [23]. We then generalize this result to the dual norm (2.9).

Theorem 4.1 (Abstract energy norm a posteriori error estimate). *Let p be the weak solution of problem (1.1a)–(1.1b) and let $p_h \in H_0^1(\Omega)$ be arbitrary. Then*

$$(4.1) \quad \|||p - p_h\||| = \inf_{\mathbf{t} \in \mathbf{H}(\text{div}, \Omega)} \sup_{\varphi \in H_0^1(\Omega), \|||\varphi\|||=1} \{ |(f - \nabla \cdot \mathbf{t}, \varphi)| + |(a\nabla p_h + \mathbf{t}, \nabla \varphi)| \}.$$

Proof. We first notice that

$$\|||p - p_h\||| = \mathcal{B} \left(p - p_h, \frac{p - p_h}{\|||p - p_h\|||} \right)$$

by (2.8). Clearly, as $\varphi := (p - p_h)/\|||p - p_h\||| \in H_0^1(\Omega)$, we immediately have $\mathcal{B}(p, \varphi) = (f, \varphi)$ by (2.7). Using this we obtain, for an arbitrary $\mathbf{t} \in \mathbf{H}(\text{div}, \Omega)$ and employing the Green theorem,

$$\begin{aligned} \mathcal{B}(p - p_h, \varphi) &= (f, \varphi) - (a\nabla p_h, \nabla \varphi) = (f, \varphi) - (a\nabla p_h + \mathbf{t}, \nabla \varphi) + (\mathbf{t}, \nabla \varphi) \\ &\leq |(f - \nabla \cdot \mathbf{t}, \varphi)| + |(a\nabla p_h + \mathbf{t}, \nabla \varphi)|. \end{aligned}$$

From here, it is enough to note that $\|||\varphi\||| = 1$ and that $\mathbf{t} \in \mathbf{H}(\text{div}, \Omega)$ was chosen arbitrary to conclude that the right-hand side term of (4.1) is an upper bound on the left-hand side one. For the converse estimate, it suffices to put $\mathbf{t} = -a\nabla p$ and to use the Cauchy–Schwarz inequality and the fact that $\|||\varphi\||| = 1$. \square

Similar arguments lead to the following corollary:

Corollary 4.2 (Abstract dual norm a posteriori error estimate). *Let the assumptions of Theorem 4.1 be verified. Then*

$$\|||p - p_h\|||_{\#} = \inf_{\mathbf{t} \in \mathbf{H}(\text{div}, \Omega)} \sup_{\varphi \in H_0^1(\Omega), \|\nabla \varphi\|=1} \{ |(f - \nabla \cdot \mathbf{t}, \varphi)| + |(a\nabla p_h + \mathbf{t}, \nabla \varphi)| \}.$$

The above theorem and corollary thus give equivalent expressions for the error.

5. GUARANTEED A POSTERIORI ERROR ESTIMATES

Our purpose is now to find computable versions of the abstract a posteriori estimates of the previous section. We first present general a posteriori error estimates, applicable to any conforming method under the condition that a suitable $\mathbf{t}_h \in \mathbf{H}(\text{div}, \Omega)$ can be found. We then propose different ways of construction of such \mathbf{t}_h for the different methods. We conclude this section by several remarks and generalizations.

5.1. General guaranteed a posteriori error estimates for conforming methods. The following is a general energy norm a posteriori error estimate for any conforming method:

Theorem 5.1 (A general guaranteed energy norm a posteriori error estimate). *Let p be the weak solution of problem (1.1a)–(1.1b) and let $p_h \in H_0^1(\Omega)$ be arbitrary. Let next $\mathcal{D}_h = \mathcal{D}_h^{\text{int}} \cup \mathcal{D}_h^{\text{ext}}$ be a partition of Ω such that $|\partial\Omega \cap \partial D| \neq 0$ for all $D \in \mathcal{D}_h^{\text{ext}}$. Let finally $\mathbf{t}_h \in \mathbf{H}(\text{div}, \Omega)$ be arbitrary but such that*

$$(5.1) \quad (\nabla \cdot \mathbf{t}_h, 1)_D = (f, 1)_D \quad \forall D \in \mathcal{D}_h^{\text{int}}.$$

Then

$$\|||p - p_h\||| \leq \left\{ \sum_{D \in \mathcal{D}_h} (\eta_{R,D} + \eta_{DF,D})^2 \right\}^{\frac{1}{2}},$$

where the diffusive flux estimator $\eta_{\text{DF},D}$ is given by

$$(5.2) \quad \eta_{\text{DF},D} := \|a^{\frac{1}{2}}\nabla p_h + a^{-\frac{1}{2}}\mathbf{t}_h\|_D \quad D \in \mathcal{D}_h,$$

and the residual estimator $\eta_{\text{R},D}$ is given by

$$(5.3) \quad \eta_{\text{R},D} := m_{D,a} \|f - \nabla \cdot \mathbf{t}_h\|_D \quad D \in \mathcal{D}_h,$$

where

$$(5.4) \quad m_{D,a}^2 := C_{\text{P},D} \frac{h_D^2}{c_{a,D}} \quad D \in \mathcal{D}_h^{\text{int}}, \quad m_{D,a}^2 := C_{\text{F},D,\partial\Omega} \frac{h_D^2}{c_{a,D}} \quad D \in \mathcal{D}_h^{\text{ext}},$$

with $C_{\text{P},D}$ the constant from the Poincaré inequality (2.4) and $C_{\text{F},D,\partial\Omega}$ the constant from the Friedrichs inequality (2.5).

Proof. Put $\mathbf{t} = \mathbf{t}_h$ in Theorem 4.1. Note that, for each $D \in \mathcal{D}_h^{\text{int}}$,

$$(f - \nabla \cdot \mathbf{t}_h, \varphi)_D = (f - \nabla \cdot \mathbf{t}_h, \varphi - \varphi_D)_D \leq \eta_{\text{R},D} \|\varphi\|_D,$$

using (5.1), the Poincaré inequality (2.4), the Cauchy–Schwarz inequality, and the definition (2.8) of the energy norm. We cannot use a similar approach also for $D \in \mathcal{D}_h^{\text{ext}}$ since there is no local conservativity supposed in (5.1) on these dual volumes. On the other hand, however, $\varphi = 0$ on $\partial D \cap \partial\Omega$, whence

$$(f - \nabla \cdot \mathbf{t}_h, \varphi)_D \leq \eta_{\text{R},D} \|\varphi\|_D$$

for each $D \in \mathcal{D}_h^{\text{ext}}$, using the Friedrichs inequality (2.5), the Cauchy–Schwarz inequality, and the definition (2.8) of the energy norm. Finally, $-(a\nabla p_h + \mathbf{t}, \nabla\varphi)_D \leq \eta_{\text{DF},D} \|\varphi\|_D$ is immediate using the fact that a is positive and scalar and the Cauchy–Schwarz inequality. Hence it now suffices to use the Cauchy–Schwarz inequality and to notice that $\|\varphi\| = 1$ in order to conclude the proof. \square

The proof of following corollary is completely similar:

Corollary 5.2 (A general guaranteed dual norm a posteriori error estimate). *Let the assumptions of Theorem 5.1 be verified. Then*

$$\| \|p - p_h\|_{\#} \leq \left\{ \sum_{D \in \mathcal{D}_h} (\eta_{\text{R},D} + \eta_{\text{DF},D})^2 \right\}^{\frac{1}{2}},$$

with the diffusive flux estimator $\eta_{\text{DF},D}$ given by

$$(5.5) \quad \eta_{\text{DF},D} := \|a\nabla p_h + \mathbf{t}_h\|_D \quad D \in \mathcal{D}_h,$$

and the residual estimator $\eta_{\text{R},D}$ given by

$$(5.6) \quad \eta_{\text{R},D} := m_D \|f - \nabla \cdot \mathbf{t}_h\|_D \quad D \in \mathcal{D}_h,$$

where

$$(5.7) \quad m_D^2 := C_{\text{P},D} h_D^2 \quad D \in \mathcal{D}_h^{\text{int}}, \quad m_D^2 := C_{\text{F},D,\partial\Omega} h_D^2 \quad D \in \mathcal{D}_h^{\text{ext}}.$$

Remark 5.3 (Assumptions of Theorem 5.1 and Corollary 5.2). Note that for Theorem 5.1 and Corollary 5.2, no additional assumptions like a polynomial form of the data, of the approximate solution, or a shape regularity of the mesh are needed.

Remark 5.4 (The mesh \mathcal{D}_h in Theorem 5.1 or Corollary 5.2). The meshes \mathcal{D}_h in Theorem 5.1 or Corollary 5.2 will differ in different types of estimates. Usually, either \mathcal{D}_h is given by the dual mesh \mathcal{D}_h , or $\mathcal{D}_h^{\text{int}} = \mathcal{S}_h$ and $\mathcal{D}_h^{\text{ext}} = \emptyset$, where \mathcal{D}_h and \mathcal{S}_h are given in Section 2.1.

In order to use Theorem 5.1 and Corollary 5.2 in practice, we need to construct a (finite-dimensional) \mathbf{t}_h satisfying (5.1). We will look for a suitable \mathbf{t}_h in the lowest-order Raviart–Thomas–Nédélec space $\mathbf{RTN}(\mathcal{S}_h)$ defined over a fine simplicial mesh \mathcal{S}_h which we suppose to be a refinement of the mesh \mathcal{D}_h from Theorem 5.1 or Corollary 5.2. The space $\mathbf{RTN}(\mathcal{S}_h) \subset \mathbf{H}(\text{div}, \Omega)$ is a space of vector functions having on each $K \in \mathcal{S}_h$ the form $(a_K + d_K x, b_K + d_K y)^t$ if $d = 2$ and $(a_K + d_K x, b_K + d_K y, c_K + d_K z)^t$ if $d = 3$. Note that the requirement $\mathbf{RTN}(\mathcal{S}_h) \subset \mathbf{H}(\text{div}, \Omega)$ imposes the continuity of the normal trace across all $\sigma \in \mathcal{G}_h^{\text{int}}$ and recall that $\mathbf{v} \cdot \mathbf{n}_\sigma$ is a constant for all $\sigma \in \mathcal{G}_h$ and that these side fluxes also represent the degrees of freedom of $\mathbf{RTN}(\mathcal{S}_h)$. For more details, we refer to [11, 33].

5.2. Constructions of the equilibrated flux \mathbf{t}_h for the vertex-centered finite volume method. We show here four different ways of constructing \mathbf{t}_h on the example of the vertex-centered finite volume method (3.4). We treat the extensions to the other methods in the following sections.

5.2.1. *Construction of \mathbf{t}_h by direct prescription.* We define $\mathbf{t}_h \in \mathbf{RTN}(\mathcal{S}_h)$ by

$$(5.8) \quad \mathbf{t}_h \cdot \mathbf{n}_\sigma = -\{a \nabla p_h \cdot \mathbf{n}_\sigma\} \quad \forall \sigma \in \mathcal{G}_h.$$

We first note that $\mathbf{t}_h \cdot \mathbf{n}_\sigma$ is given directly by $-a \nabla p_h \cdot \mathbf{n}_\sigma$ for such $\sigma \in \mathcal{G}_h$ which are in the interior of some $K \in \mathcal{T}_h$ (where a and ∇p_h are constant) or at the boundary of Ω ; a simple averaging is used otherwise. We have the following key result:

Lemma 5.5 (Reconstructed diffusion residual for the vertex-centered finite volume method). *Let $p_h \in X_h^0$ be given by the vertex-centered finite volume method (3.4). Let \mathbf{t}_h be given by (5.8). Then (5.1) holds true.*

Proof. The local conservativity of the vertex-centered finite volume method (3.4) and the definition (5.8) of \mathbf{t}_h imply that

$$\langle \mathbf{t}_h \cdot \mathbf{n}, 1 \rangle_{\partial D} = (f, 1)_D \quad \forall D \in \mathcal{D}_h^{\text{int}}.$$

The assertion of the lemma follows by the Green theorem. \square

Consequently, \mathbf{t}_h given by (5.8) can be used in Theorem 5.1 and Corollary 5.2 with \mathcal{D}_h being the dual mesh of the vertex-centered finite volume method (3.4). Such an estimate, however, may suffer from two inconveniences. Whenever $D \in \mathcal{D}_h^{\text{int}}$ is nonconvex, the Poincaré constant $C_{P,D}$ from (2.4) is no longer equal to $1/\pi^2$ and its evaluation is much more difficult leading to less sharp estimates. The second inconvenience was pointed out in [14]: as (5.1) only holds on a set of elements \mathcal{S}_D and not on each $K \in \mathcal{S}_h$, the contribution of the residual estimators may dominate the diffusive flux ones, not being a higher-order term as in [41, 43, 18], and the effectivity index does not approach the optimal value of one. The approaches of the three following sections improve on these two points (we present them in the energy norm setting, similar results in the dual norm setting are rather straightforward).

5.2.2. *Construction of \mathbf{t}_h by local minimization involving local linear systems solution.* In [14], $\mathbf{t}_h \cdot \mathbf{n}_\sigma$ is given by (5.8) only on such $\sigma \in \mathcal{G}_h$ which are at the boundary of some $D \in \mathcal{D}_h^{\text{int}}$. By the Green theorem, this guarantees (5.1) as in Lemma 5.5. The remaining sides lie in the interior of some $D \in \mathcal{D}_h$ (or at the boundary of Ω), so that $\mathbf{t}_h \cdot \mathbf{n}_\sigma$ can be chosen locally and independently by local minimization of $\eta_{R,D}^2 + \eta_{DF,D}^2$ for each $D \in \mathcal{D}_h$. This leads to a solution of a small linear system for each $D \in \mathcal{D}_h$ and helps to improve the effectivity index to a value close to one.

5.2.3. *Construction of \mathbf{t}_h by local minimization without local linear systems solution.* We suggest here an improvement which avoids any local systems solution.

Let $D \in \mathcal{D}_h$ be fixed. The first step is to construct $\mathbf{t}_{1,D} \in \mathbf{RTN}(\mathcal{S}_D)$ given by (5.8). In the second one, we then construct $\mathbf{t}_{2,D} \in \mathbf{RTN}(\mathcal{S}_D)$ given by (5.8) only for such $\sigma \in \mathcal{G}_h$ contained in D which are at the boundary of some $E \in \mathcal{D}_h^{\text{int}}$ and such that $(\nabla \cdot \mathbf{t}_{2,D}, 1)_K = (f, 1)_K$ for all $K \in \mathcal{S}_D$. Note that as $(\nabla \cdot \mathbf{t}_{2,D}, 1)_D = \langle \mathbf{t}_{2,D} \cdot \mathbf{n}, 1 \rangle_{\partial D} = (f, 1)_D$ when $D \in \mathcal{D}_h^{\text{int}}$, this can be done without any (local) linear system solution by choosing the flux over one interior side and a sequential construction as $\sum_{K \in \mathcal{S}_D} (f, 1)_K = (f, 1)_D$. If $D \in \mathcal{D}_h^{\text{ext}}$, this argument is then replaced by the fact that we are free to choose the fluxes over the exterior sides. Now any $\mathbf{t}_D := \alpha \mathbf{t}_{1,D} + (1 - \alpha) \mathbf{t}_{2,D}$ obviously obeys (5.1) and we can minimize $\eta_D := \eta_{R,D} + \eta_{DF,D}$ as a function of the parameter α . It turns out that it is much easier to minimize $\eta_{R,D}^2 + \eta_{DF,D}^2$, as this is a quadratic function of α , and the optimal value is easily found to be given by

$$\begin{aligned} & \alpha (\|a^{-\frac{1}{2}}(\mathbf{t}_{1,D} - \mathbf{t}_{2,D})\|_D^2 + m_{D,a}^2 \|\nabla \cdot (\mathbf{t}_{1,D} - \mathbf{t}_{2,D})\|_D^2) \\ &= -(a^{\frac{1}{2}} \nabla p_h + a^{-\frac{1}{2}} \mathbf{t}_{2,D}, a^{-\frac{1}{2}}(\mathbf{t}_{1,D} - \mathbf{t}_{2,D}))_D \\ & \quad + m_{D,a}^2 (f - \nabla \cdot \mathbf{t}_{2,D}, \nabla \cdot (\mathbf{t}_{1,D} - \mathbf{t}_{2,D}))_D. \end{aligned}$$

As however this value does not necessarily minimize η_D (when it is uniquely defined by the above formula) but $\eta_{R,D}^2 + \eta_{DF,D}^2$, we finally propose as an improved estimator

$$(5.9) \quad \eta_D := \min\{\eta_D(\mathbf{t}_{1,D}), \eta_D(\mathbf{t}_{2,D}), \eta_D(\alpha \mathbf{t}_{1,D} + (1 - \alpha) \mathbf{t}_{2,D})\}.$$

Such an estimator will be locally efficient (and robust) whenever it is the case for $\eta_D(\mathbf{t}_{1,D})$. Hence, in Section 6 below, we only prove the efficiency for $\eta_D(\mathbf{t}_{1,D})$.

5.2.4. *Construction of \mathbf{t}_h by mixed finite element approximations of local Neumann/Dirichlet problems.* We adapt here to the present setting the approach of [19]. For a given $D \in \mathcal{D}_h$, let

$$\mathbf{RTN}_N(\mathcal{S}_D) = \{\mathbf{v}_h \in \mathbf{RTN}(\mathcal{S}_D); \mathbf{v}_h \cdot \mathbf{n}_\sigma = -\{a \nabla p_h \cdot \mathbf{n}_\sigma\} \quad \forall \sigma \in \mathcal{G}_h^{\text{int}} \cap \partial D\}.$$

Let f_h be given by $(f, 1)_K / |K|$ for all $K \in \mathcal{S}_h$. We then define $\mathbf{t}_h \in \mathbf{RTN}(\mathcal{S}_h)$ by solving on each $D \in \mathcal{D}_h$ the following minimization problem:

$$(5.10) \quad \mathbf{t}_h|_D = \arg \inf_{\mathbf{v}_h \in \mathbf{RTN}_N(\mathcal{S}_D), \nabla \cdot \mathbf{v}_h = f_h} \|a^{\frac{1}{2}} \nabla p_h + a^{-\frac{1}{2}} \mathbf{v}_h\|_D.$$

Define $\mathbf{RTN}_{N,0}(\mathcal{S}_D)$ as $\mathbf{RTN}_N(\mathcal{S}_D)$ but with the normal flux condition $\mathbf{v}_h \cdot \mathbf{n}_\sigma = 0$. Let $\mathbb{P}_0^*(\mathcal{S}_D)$ be spanned by piecewise constants on \mathcal{S}_D with zero mean on D when $D \in \mathcal{D}_h^{\text{int}}$; when $D \in \mathcal{D}_h^{\text{ext}}$, the mean value condition is not imposed. Then it is easy to show that (5.10) is equivalent to finding $\mathbf{t}_h \in \mathbf{RTN}_N(\mathcal{S}_D)$ and $q_h \in \mathbb{P}_0^*(\mathcal{S}_D)$, the mixed finite element approximations of local Neumann problems on $D \in \mathcal{D}_h^{\text{int}}$ and local Neumann/Dirichlet problems on $D \in \mathcal{D}_h^{\text{ext}}$:

$$(5.11a) \quad (a^{-1} \mathbf{t}_h + \nabla p_h, \mathbf{v}_h)_D - (q_h, \nabla \cdot \mathbf{v}_h)_D = 0 \quad \forall \mathbf{v}_h \in \mathbf{RTN}_{N,0}(\mathcal{S}_D),$$

$$(5.11b) \quad (\nabla \cdot \mathbf{t}_h, \phi_h)_D = (f, \phi_h)_D \quad \forall \phi_h \in \mathbb{P}_0^*(\mathcal{S}_D).$$

Note in particular that the function $-\{a \nabla p_h \cdot \mathbf{n}_\sigma\}$ on the boundary of each $D \in \mathcal{D}_h^{\text{int}}$ by (3.4) satisfies the compatibility condition, whence also the existence and uniqueness follow. Theorem 5.1 and Corollary 5.2 are to be used here with $\mathcal{D}_h^{\text{int}} = \mathcal{S}_h$ and $\mathcal{D}_h^{\text{ext}} = \emptyset$. A solution of a local linear system on each $D \in \mathcal{D}_h$ is necessary but the results of Section 7 below reveal excellent.

5.3. Construction of the equilibrated flux \mathbf{t}_h for the weighted vertex-centered finite volume method. In the spirit of the previous section, we show here one particular way of constructing a suitable $\mathbf{t}_h \in \mathbf{RTN}(\mathcal{S}_h)$ for the weighted vertex-centered finite volume method (3.5). We simply define $\mathbf{t}_h \in \mathbf{RTN}(\mathcal{S}_h)$ by

$$(5.12) \quad \mathbf{t}_h \cdot \mathbf{n}_\sigma = -\{ \{ a \nabla p_h \cdot \mathbf{n}_\sigma \} \}_\omega \quad \forall \sigma \in \mathcal{G}_h.$$

For the moment, we do not specify the weights in (5.12), but it will turn out that the choice (3.3) will lead to fully robust energy norm a posteriori error estimates. The following is the equivalent of Lemma 5.5 in the present setting:

Lemma 5.6 (Reconstructed diffusion residual for the weighted vertex-centered finite volume method). *Let $p_h \in X_h^0$ be given by the weighted vertex-centered finite volume method (3.5), with any weights satisfying (2.2). Let \mathbf{t}_h be given by (5.12), where the weights in (5.12) are the same as those used in (3.5) for all $\sigma \in \mathcal{F}_h^{\text{int}}$ if a is discontinuous and piecewise constant on \mathcal{D}_h . If a is piecewise constant on \mathcal{T}_h (comprising the case $a = 1$), let the weights in (5.12) be arbitrary but satisfying (2.2). Then (5.1) holds true.*

5.4. Guaranteed estimates for the finite element method. Recall from Corollary 3.12 that whenever f is piecewise constant on \mathcal{T}_h , the a posteriori error estimates for the finite element method (3.6) can be obtained by any of the approaches of Section 5.2. For general f , let f_h be given by $(f, 1)_K/|K|$ on all $K \in \mathcal{T}_h$. Following [34], we then have:

Theorem 5.7 (Guaranteed a posteriori error estimate for the finite element method). *Let p be the weak solution of problem (1.1a)–(1.1b), let p_h be its finite element approximation given by (3.6), let \tilde{p} be the weak solution of problem (1.1a)–(1.1b) with f replaced by f_h , and let \tilde{p}_h be its finite element approximation. Then*

$$\| \| p - p_h \| \| \leq \| \| \tilde{p} - \tilde{p}_h \| \| + 2 \left\{ \sum_{K \in \mathcal{T}_h} \eta_{\text{Osc}, K}^2 \right\}^{\frac{1}{2}},$$

where

$$\eta_{\text{Osc}, K} := C_{\text{P}, K}^{\frac{1}{2}} \frac{h_K}{c_{a, K}^{\frac{1}{2}}} \| f - f_K \|_K \quad K \in \mathcal{T}_h.$$

Proof. The triangle inequality implies

$$\| \| p - p_h \| \| \leq \| \| p - \tilde{p} \| \| + \| \| \tilde{p} - \tilde{p}_h \| \| + \| \| \tilde{p}_h - p_h \| \|.$$

By the same reasoning as in the proof of Theorem 4.1, using the definitions of the weak solutions, and finally similarly as in the proof of Theorem 5.1,

$$\begin{aligned} \| \| p - \tilde{p} \| \| &= \sup_{\varphi \in H_0^1(\Omega), \| \varphi \| = 1} (a \nabla(p - \tilde{p}), \nabla \varphi) = \sup_{\varphi \in H_0^1(\Omega), \| \varphi \| = 1} (f - f_h, \varphi) \\ &\leq \sup_{\varphi \in H_0^1(\Omega), \| \varphi \| = 1} \sum_{K \in \mathcal{T}_h} (f - f_K, \varphi - \varphi_K)_K \leq \left\{ \sum_{K \in \mathcal{T}_h} \eta_{\text{Osc}, K}^2 \right\}^{\frac{1}{2}}. \end{aligned}$$

Estimating the term $\| \| \tilde{p}_h - p_h \| \|$ similarly in a discrete setting concludes the proof. \square

The version of Theorem 5.7 for the dual norm $\| \| \cdot \| \|_{\#}$ is obvious.

5.5. Remarks and generalizations.

Remark 5.8 (Comparison with standard residual estimators). The above estimates have three basic advantages in comparison with standard residual estimators, cf. Verfürth [38]. First of all, they feature no undetermined constant and deliver a guaranteed upper bound. We remark however that defining \mathbf{t}_h by (5.8), the evaluation of the constants $C_{P,D}$ and $C_{F,D,\partial\Omega}$ is necessary, which is only straightforward when $D \in \mathcal{D}_h^{\text{int}}$ are convex and $D \in \mathcal{D}_h^{\text{ext}}$ have suitable form, see Section 2.3. Thus the approach of Section 5.2.4 (or that of Section 5.2.3 with $\mathbf{t}_{2,D}$ only), where $C_{P,D} = 1/\pi^2$ and $C_{F,D,\partial\Omega}$ does not appear at all, seems preferable. Next, the classical residual estimator $h_K \|f\|_K$ is replaced by its improved version (5.3). Lastly, as it will be seen in Section 6 below, our estimates represent local lower bounds for the classical residual estimators. The improved behavior of our estimators over the classical one for the finite element method is numerically studied in [14].

Remark 5.9 (Comparison with the equilibrated residual method). In the equilibrated residual method, cf. [3], one searches equilibrated fluxes expressing local conservativity over each $K \in \mathcal{T}_h$, by means of solution of local linear systems. Contrarily to this approach, our estimators are based on the immediately available conservativity of the finite element method over the dual grids \mathcal{D}_h . We remark that we obtain immediately a guaranteed and locally computable upper bound. This is also possible in the approach of [3] if the data oscillation term is separated, cf. [2].

Remark 5.10 (Comparison with the Zienkiewicz–Zhu averaging). The similarity of our approach with the Zienkiewicz–Zhu [46] estimator relies in the fact that both contain what we call a diffusive flux estimator, where \mathbf{t}_h is produced from $-\nabla p_h$ by averaging. Concerning the differences, first of all, in the Zienkiewicz–Zhu estimator, one averages punctual nodal values and the postprocessed diffusive flux \mathbf{t}_h is smooth (belongs to C^0). According to Theorem 4.1, there is, however, no need for this—only normal traces of \mathbf{t}_h should be continuous, i.e., $\mathbf{t}_h \in \mathbf{H}(\text{div}, \Omega)$ is enough, which is achieved in our approach by averaging the side normal components. Secondly, this estimator does not give a guaranteed upper bound since in particular the residual part (5.3) is omitted. Thirdly, these two differences become fundamentally important when a is discontinuous. The flux \mathbf{t}_h then has to be produced from $-a\nabla p_h$ and not from $-\nabla p_h$ and also the weaker regularity $\mathbf{t}_h \in \mathbf{H}(\text{div}, \Omega)$ is optimal, as $-a\nabla p$ is not smooth and only belongs to $\mathbf{H}(\text{div}, \Omega)$. Also, the residual parts play a crucial role through the presence of the material coefficient $c_{a,D}^{\frac{1}{2}}$, see also the discussion in [21].

Remark 5.11 (Comparison with functional a posteriori estimates). Repin [31] or Korotov [22] use instead of Theorem 5.1 the estimate

$$\| \|p - p_h\| \| \leq \frac{C_{F,\Omega}^{1/2} h_\Omega}{c_{a,\Omega}^{1/2}} \|f - \nabla \cdot \mathbf{t}_h\| + \|a^{\frac{1}{2}} \nabla p_h + a^{-\frac{1}{2}} \mathbf{t}_h\|,$$

which follows readily from Theorem 4.1 using the Cauchy–Schwarz inequality, the Friedrichs inequality, and the definition of the energy seminorm. Here p is the weak solution given by (2.7), $p_h \in H_0^1(\Omega)$ and $\mathbf{t}_h \in \mathbf{H}(\text{div}, \Omega)$ are arbitrary, $C_{F,\Omega}$ is the constant from the Friedrichs inequality (2.5) with $D = \Omega$, and h_Ω is the diameter of Ω . The advantage is that no particular construction of $\mathbf{t}_h \in \mathbf{H}(\text{div}, \Omega)$ has to be done and the estimate is thus fully scheme-independent. However, as

no information from the computation is used, the residual term is in general too large by the presence of h_Ω instead of h_D which we find in Theorem 5.1. Secondly, the term $1/c_{a,\Omega}^{1/2}$ is also greatly unfavorable in comparison with $1/c_{a,D}^{1/2}$ found in our estimates. Thus, a rather expensive global minimization is usually employed in the type of estimates of [31] or [22].

Remark 5.12 (Comparison with the estimator of Luce and Wohlmuth [26]). Our estimators are similar to those of Luce and Wohlmuth [26], in particular in that we construct the dual mesh \mathcal{D}_h and the second simplicial triangulation \mathcal{S}_h and a $\mathbf{t}_h \in \text{RTN}(\mathcal{S}_h)$. However, in particular the construction of \mathbf{t}_h by (5.12), as shown below, leads to full robustness with respect to discontinuous coefficients in the energy norm.

Remark 5.13 (Residual estimators and data oscillation). Note that whenever $f \in H^1(K)$ for all $K \in \mathcal{S}_h$, the residual estimators $\eta_{R,D}$ in Section 5.2.4 (or those of Section 5.2.3 with $\mathbf{t}_{2,D}$ only) represent a contribution of higher order, as $\|f - f_h\|_K \leq 1/\pi h_K \|\nabla f\|_K$ by the Poincaré inequality (2.4) (using the convexity of simplices). Moreover, if f is piecewise constant on \mathcal{S}_h , they disappear completely.

Remark 5.14 (Generalizations to other methods). The above a posteriori error estimates may be generalized easily to other methods discussed in Section 3 using the equivalence results stated therein.

6. EFFICIENCY AND ROBUSTNESS OF THE A POSTERIORI ERROR ESTIMATES

We prove here the (local) efficiency and robustness of our estimates. We first present a robustness energy norm result for the weighted vertex-centered finite volume method (3.5). Then robustness in the dual norm for all the considered methods is proven. Finally, some generalizations are discussed.

6.1. Local efficiency and robustness of the energy norm a posteriori error estimate for weighted vertex-centered finite volumes. The result of this section is given in the energy norm (2.8) and only applies to the harmonic-weighted vertex-centered finite volume method (3.5).

Theorem 6.1 (Local efficiency and robustness of the energy norm a posteriori error estimate for the weighted vertex-centered finite volume method). *Let a be piecewise constant on \mathcal{D}_h , let f be a piecewise polynomial of degree m on \mathcal{S}_h , let p be the weak solution of problem (1.1a)–(1.1b), and let p_h be its weighted vertex-centered finite volume approximation (3.5), with the weights (3.3). Let next \mathcal{S}_h be shape-regular with the constant κ_S and let \mathbf{t}_h be given by (5.12) with the weights (3.3), $\eta_{DF,D}$ given by (5.2), and $\eta_{R,D}$ by (5.3). Then, for each $D \in \mathcal{D}_h$, there holds*

$$(6.1a) \quad \eta_{DF,D} \leq C \| \|p - p_h\| \|_{\mathcal{T}_{V_D}},$$

$$(6.1b) \quad \eta_{R,D} \leq \tilde{C} \| \|p - p_h\| \|_{\mathcal{T}_{V_D}},$$

where the constant C depends only on d , κ_S , and m and \tilde{C} in addition depends on $C_{P,D}$ if $D \in \mathcal{D}_h^{\text{int}}$ or $C_{F,D,\partial\Omega}$ if $D \in \mathcal{D}_h^{\text{ext}}$.

The proof of Theorem 6.1 is decomposed into two parts. For $\eta_{DF,D}$, Lemma 6.2 shows that the construction (5.12) implies that the normal components of \mathbf{t}_h differ from those of $a\nabla p_h$ by the jumps of $a\nabla p_h \cdot \mathbf{n}$. The latter are a part of residual estimators and are therefore known to be bounded by the error. The second estimator, $\eta_{R,D}$, is then efficient due to a complementarity argument as shown in Lemma 6.3.

Lemma 6.2 (Local efficiency of the diffusive flux estimator). *Let the assumptions of Theorem 6.1 be verified. Then (6.1a) holds true.*

Proof. The proof follows the techniques of [38] and [18]. Recall first the standard estimate

$$(6.2) \quad \|\mathbf{v}_h\|_K^2 \leq Ch_K \sum_{\sigma \in \mathcal{E}_K} \|\mathbf{v}_h \cdot \mathbf{n}\|_\sigma^2$$

valid for each $\mathbf{v}_h \in \mathbf{RTN}(K)$ and any simplex K . Here, and similarly in the rest of the proof, the constant C , not necessarily the same at each occurrence, depends only on d , κ_S , and m .

Let now K be an arbitrary element in the simplicial mesh \mathcal{S}_D of a given $D \in \mathcal{D}_h$ and let us put $\mathbf{v}_h = a\nabla p_h + \mathbf{t}_h$. We have

$$(6.3) \quad \|a^{\frac{1}{2}}\nabla p_h + a^{-\frac{1}{2}}\mathbf{t}_h\|_K^2 = a_K^{-1}\|\mathbf{v}_h\|_K^2 \leq Ca_K^{-1}h_K \sum_{\sigma \in \mathcal{E}_K \cap \mathcal{G}_h^{\text{int}}} \|\omega_{L,\sigma} [a\nabla p_h \cdot \mathbf{n}_\sigma]\|_\sigma^2,$$

where L denotes the neighboring element to K across $\sigma \in \mathcal{G}_h^{\text{int}}$, using that

$$(6.4) \quad (a\nabla p_h + \mathbf{t}_h)|_K \cdot \mathbf{n}_\sigma = (a\nabla p_h \cdot \mathbf{n}_\sigma)|_K - \{a\nabla p_h \cdot \mathbf{n}_\sigma\}_\omega = \mathbf{n}_\sigma \cdot \mathbf{n} \omega_{L,\sigma} [a\nabla p_h \cdot \mathbf{n}_\sigma]$$

for $\sigma \in \mathcal{E}_K \cap \mathcal{G}_h^{\text{int}}$ and $(a\nabla p_h + \mathbf{t}_h)|_K \cdot \mathbf{n}_\sigma = 0$ for $\sigma \in \mathcal{E}_K \cap \mathcal{G}_h^{\text{ext}}$. Note that $\mathbf{n}_\sigma \cdot \mathbf{n} = \pm 1$ is only used as a sign determination.

Let us now consider a fixed $\sigma = \sigma_{K,L} \in \mathcal{E}_K \cap \mathcal{G}_h^{\text{int}}$. The estimate

$$h_K^{\frac{1}{2}} \|[a\nabla p_h \cdot \mathbf{n}_\sigma]\|_\sigma \leq C \sum_{M \in \{K,L\}} a_M^{\frac{1}{2}} \|p - p_h\|_M.$$

is standard using the side and element bubble functions, the Green theorem, the inverse inequality, and the equivalence of norms on finite-dimensional spaces, cf. [38]. It then follows that

$$\omega_{L,\sigma} a_K^{-\frac{1}{2}} h_K^{\frac{1}{2}} \|[a\nabla p_h \cdot \mathbf{n}_\sigma]\|_\sigma \leq C \sum_{M \in \{K,L\}} \omega_{L,\sigma} a_K^{-\frac{1}{2}} a_M^{\frac{1}{2}} \|p - p_h\|_M.$$

Finally, thanks to the definition (2.2) of $\omega_{L,\sigma}$, $\omega_{L,\sigma} a_K^{-\frac{1}{2}} a_M^{\frac{1}{2}} = \omega_{L,\sigma} \leq 1$ if $M = K$ and by (3.3), $\omega_{L,\sigma} a_K^{-\frac{1}{2}} a_M^{\frac{1}{2}} = a_K(a_K + a_L)^{-1} a_K^{-\frac{1}{2}} a_L^{\frac{1}{2}} \leq \frac{1}{2}$ if $M = L$, using the inequality $2ab \leq a^2 + b^2$.

Now finally, using the above results,

$$\begin{aligned} \eta_{\text{DF},D}^2 &= \sum_{K \in \mathcal{S}_D} \|a^{\frac{1}{2}}\nabla p_h + a^{-\frac{1}{2}}\mathbf{t}_h\|_K^2 \\ &\leq C \sum_{K \in \mathcal{S}_D} \sum_{\sigma_{K,L} \in \mathcal{E}_K \cap \mathcal{G}_h^{\text{int}}} a_K^{-1} h_K \omega_{L,\sigma_{K,L}}^2 \|[a\nabla p_h \cdot \mathbf{n}_{\sigma_{K,L}}]\|_{\sigma_{K,L}}^2 \\ &\leq C \sum_{K \in \mathcal{S}_D} \sum_{\sigma_{K,L} \in \mathcal{E}_K \cap \mathcal{G}_h^{\text{int}}} \sum_{M \in \{K,L\}} \|p - p_h\|_M^2 \leq C \|p - p_h\|_{T_{V_D}}^2, \end{aligned}$$

which was to be proved. \square

Lemma 6.3 (Local efficiency of the residual estimator). *Let the assumptions of Theorem 6.1 be verified. Then (6.1b) holds true.*

Proof. Let us consider a fixed $D \in \mathcal{D}_h$. First,

$$\|f - \nabla \cdot \mathbf{t}_h\|_K \leq C a_K^{\frac{1}{2}} h_K^{-1} \|a^{\frac{1}{2}} \nabla p + a^{-\frac{1}{2}} \mathbf{t}_h\|_K$$

for each $K \in \mathcal{S}_D$ with C depending only on d, κ_S , and m follows standardly by using the element bubble function, the equivalence of norms on finite-dimensional spaces, definition (2.7) of the weak solution, the Green theorem, the Cauchy–Schwarz inequality, definition (2.8) of the energy norm, and the inverse inequality, cf. [38] or [41, Lemma 7.6]. Hence

$$\|f - \nabla \cdot \mathbf{t}_h\|_D \leq C C_{a,D}^{\frac{1}{2}} h_D^{-1} \|a^{\frac{1}{2}} \nabla p + a^{-\frac{1}{2}} \mathbf{t}_h\|_D$$

holds true, using also the fact that $h_D / \min_{K \in \mathcal{S}_D} h_K$ is bounded by the shape-regularity of \mathcal{S}_h . Thus

$$h_D c_{a,D}^{-\frac{1}{2}} \|f - \nabla \cdot \mathbf{t}_h\|_D \leq C c_{a,D}^{-\frac{1}{2}} C_{a,D}^{\frac{1}{2}} \|a^{\frac{1}{2}} \nabla p + a^{-\frac{1}{2}} \mathbf{t}_h\|_D.$$

Next note that $c_{a,D}^{-\frac{1}{2}} C_{a,D}^{\frac{1}{2}} = 1$ for a piecewise constant on \mathcal{D}_h . Finally,

$$\|a^{\frac{1}{2}} \nabla p + a^{-\frac{1}{2}} \mathbf{t}_h\|_D \leq \|p - p_h\|_D + \|a^{\frac{1}{2}} \nabla p_h + a^{-\frac{1}{2}} \mathbf{t}_h\|_D$$

using the triangle inequality, which concludes the proof by virtue of the previously proved estimate (6.1a). \square

6.2. Global efficiency and robustness of the dual norm a posteriori error estimates. The result of this section is given in the dual norm (2.9) and applies to all the methods studied in this paper. It is based on the direct prescription of \mathbf{t}_h by (5.8) or (5.12). Similar result based on the approach of Section 5.2.4 is possible.

Theorem 6.4 (Global efficiency and robustness of the dual norm a posteriori error estimates). *Let f be a piecewise polynomial of degree m on \mathcal{S}_h , let p be the weak solution of problem (1.1a)–(1.1b), and let $p_h \in X_h^0$ be arbitrary. Let next \mathcal{S}_h be shape-regular with the constant κ_S and let \mathbf{t}_h be given by (5.12) with any weights satisfying (2.2), $\eta_{\text{DF},D}$ by (5.5), and $\eta_{\text{R},D}$ by (5.6). Then, there holds*

$$(6.5) \quad \left\{ \sum_{D \in \mathcal{D}_h} (\eta_{\text{DF},D} + \eta_{\text{R},D})^2 \right\}^{\frac{1}{2}} \leq C \|p - p_h\|_{\#},$$

where the constant C depends only on d, κ_S, m , and $C_{\text{P},D}$ for $D \in \mathcal{D}_h^{\text{int}}$ and $C_{\text{F},D,\partial\Omega}$ for $D \in \mathcal{D}_h^{\text{ext}}$.

Proof. Throughout this proof, C denotes a generic constant with the dependencies indicated in the announcement, possibly different at different occurrences. Let $K \in \mathcal{S}_D, D \in \mathcal{D}_h$ be given. Adding and subtracting $\nabla \cdot (a \nabla p_h)$, using the triangle inequality, the fact that $h_D \leq C h_K$, and the inverse inequality, we have

$$\begin{aligned} C_{\text{P},D}^{\frac{1}{2}} h_D \|f - \nabla \cdot \mathbf{t}_h\|_K &\leq C_{\text{P},D}^{\frac{1}{2}} h_D (\|f + \nabla \cdot (a \nabla p_h)\|_K + \|\nabla \cdot (a \nabla p_h + \mathbf{t}_h)\|_K) \\ &\leq C h_K \|f + \nabla \cdot (a \nabla p_h)\|_K + C \|a \nabla p_h + \mathbf{t}_h\|_K. \end{aligned}$$

Using (6.2), (5.12), (6.4), and (2.2), we obtain

$$\|a \nabla p_h + \mathbf{t}_h\|_K^2 \leq C h_K \sum_{\sigma \in \mathcal{E}_K \cap \mathcal{G}_h^{\text{int}}} \|[a \nabla p_h \cdot \mathbf{n}_\sigma]\|_\sigma^2$$

(note that in both cases that a is piecewise constant on \mathcal{T}_h or that a is piecewise constant on \mathcal{D}_h , a is piecewise constant on \mathcal{S}_h). Combining the two above estimates,

$$\sum_{D \in \mathcal{D}_h} (\eta_{\text{DF},D} + \eta_{\text{R},D})^2 \leq C \left(\sum_{K \in \mathcal{S}_h} h_K^2 \|f + \nabla \cdot (a \nabla p_h)\|_K^2 + \sum_{\sigma \in \mathcal{G}_h^{\text{int}}} h_\sigma \| [a \nabla p_h \cdot \mathbf{n}_\sigma] \|_\sigma^2 \right).$$

Note that this means that the present estimates represent a lower bound for the standard residual ones (cf. [38]). The rest of the proof is based on the tools from [39].

We next prove that

$$(6.6) \quad \left\{ \sum_{K \in \mathcal{S}_h} h_K^2 \|f + \nabla \cdot (a \nabla p_h)\|_K^2 \right\}^{\frac{1}{2}} \leq C \|p - p_h\|_\#.$$

Let $K \in \mathcal{S}_h$. Denote by ψ_K the element bubble function (cf. [38]) and put $v_K := (f + \nabla \cdot (a \nabla p_h))|_K$. By the equivalence of norms on finite-dimensional spaces, properties of the bubble functions, and definition (2.7) of the weak solution, we have, cf. [38],

$$\|v_K\|_K^2 \leq C (a \nabla(p - p_h), \nabla(\psi_K v_K))_K.$$

Next, by the inverse inequality and the properties of the bubble functions,

$$h_K^2 \|\nabla(\psi_K v_K)\|_K \leq C h_K \|v_K\|_K.$$

Put $\lambda|_K = h_K^2 \psi_K v_K$ and note that $\lambda \in H_0^1(\Omega)$. Using the two above inequalities,

$$\begin{aligned} \sum_{K \in \mathcal{S}_h} h_K^2 \|v_K\|_K^2 &\leq C \sum_{K \in \mathcal{S}_h} h_K^2 (a \nabla(p - p_h), \nabla(\psi_K v_K))_K = C \frac{\mathcal{B}(p - p_h, \lambda)}{\|\nabla \lambda\|} \|\nabla \lambda\| \\ &\leq C \|p - p_h\|_\# \left\{ \sum_{K \in \mathcal{S}_h} h_K^4 \|\nabla(\psi_K v_K)\|_K^2 \right\}^{\frac{1}{2}} \\ &\leq C \|p - p_h\|_\# \left\{ \sum_{K \in \mathcal{S}_h} h_K^2 \|v_K\|_K^2 \right\}^{\frac{1}{2}} \end{aligned}$$

employing also the definition (2.9) of the dual norm and the Cauchy–Schwarz inequality. Thus (6.6) is proved.

The final point of the proof is to show that

$$(6.7) \quad \left\{ \sum_{\sigma \in \mathcal{G}_h^{\text{int}}} h_\sigma \| [a \nabla p_h \cdot \mathbf{n}_\sigma] \|_\sigma^2 \right\}^{\frac{1}{2}} \leq C \|p - p_h\|_\#.$$

For $\sigma \in \mathcal{G}_h^{\text{int}}$, put $v|_\sigma := [a \nabla p_h \cdot \mathbf{n}_\sigma]$; we keep the same notation for the lifting of $v|_\sigma$ to the two simplices K and L sharing the side σ . Let ψ_σ be the face bubble function (cf. once again [38]). Then there holds

$$\|v_\sigma\|_\sigma^2 \leq C \langle v_\sigma, \psi_\sigma v_\sigma \rangle_\sigma,$$

$$\|\psi_\sigma v_\sigma\|_K \leq C h_\sigma^{\frac{1}{2}} \|v_\sigma\|_\sigma.$$

Put $\lambda := \sum_{\sigma \in \mathcal{G}_h^{\text{int}}} h_\sigma \psi_\sigma v_\sigma$. Note that $\lambda \in H_0^1(\Omega)$, as only the interior sides appear in the sum. Finally, note that by the second of the above inequalities,

$$\|\lambda\|_K \leq \sum_{\sigma \in \mathcal{E}_K \cap \mathcal{G}_h^{\text{int}}} h_\sigma \|\psi_\sigma v_\sigma\|_K \leq C \sum_{\sigma \in \mathcal{E}_K \cap \mathcal{G}_h^{\text{int}}} h_\sigma^{\frac{3}{2}} \|v_\sigma\|_\sigma.$$

Using the above inequalities and the Green theorem,

$$\begin{aligned}
 & \sum_{\sigma \in \mathcal{G}_h^{\text{int}}} h_\sigma \|v_\sigma\|_\sigma^2 \\
 \leq & C \sum_{\sigma \in \mathcal{G}_h^{\text{int}}} \langle [a \nabla p_h \cdot \mathbf{n}_\sigma], \lambda \rangle_\sigma = C \sum_{K \in \mathcal{S}_h} \{ (f + \nabla \cdot (a \nabla p_h), \lambda)_K - (a \nabla(p - p_h), \nabla \lambda)_K \} \\
 \leq & C \|p - p_h\|_{\#} \|\nabla \lambda\| + C \left\{ \sum_{K \in \mathcal{S}_h} h_K^2 \|f + \nabla \cdot (a \nabla p_h)\|_K^2 \right\}^{\frac{1}{2}} \left\{ \sum_{K \in \mathcal{S}_h} h_K^{-2} \|\lambda\|_K^2 \right\}^{\frac{1}{2}} \\
 \leq & C \|p - p_h\|_{\#} \left\{ \sum_{K \in \mathcal{S}_h} h_K^{-2} \|\lambda\|_K^2 \right\}^{\frac{1}{2}} \leq C \|p - p_h\|_{\#} \left\{ \sum_{\sigma \in \mathcal{G}_h^{\text{int}}} h_\sigma \|v_\sigma\|_\sigma^2 \right\}^{\frac{1}{2}},
 \end{aligned}$$

where we have also employed (6.6), the inverse inequality, and the Cauchy–Schwarz inequality. Thus (6.7) is proved. \square

6.3. Remarks and generalizations. We conclude this section by several remarks and comments on generalizations.

Remark 6.5 (Unconditioned energy norm robustness with respect to discontinuous a). When a is piecewise constant on \mathcal{D}_h , when the harmonic averaging (3.3) has been used in the weighted vertex-centered finite volume method (3.5), and when the diffusive flux \mathbf{t}_h is likewise defined using harmonic averaging (3.3), equations (6.1a)–(6.1b) imply a full robustness of the estimators of Theorem 5.1 with respect to the diffusion coefficient a . In particular, no condition on the spatial distribution of the discontinuities in a is necessary, whereas in the previous results [9, 28, 16, 1], a ‘monotonicity around vertices’ condition or a similar assumption on the distribution of the diffusion coefficient was always necessary.

Remark 6.6 (Diffusion coefficient a piecewise constant on \mathcal{T}_h). If a is piecewise constant on \mathcal{T}_h (whence the choice of the weights does not influence (3.5), cf. Remark 3.4) but harmonic averaging (3.3) has been used in order to define the diffusive flux \mathbf{t}_h in (5.12), equation (6.1a) still holds true, i.e., the diffusive flux estimator $\eta_{\text{DF},D}$ is still fully robust. It however follows from the proof of Lemma 6.3 that in equation (6.1b), an additional factor $c_{a,D}^{-\frac{1}{2}} C_{a,D}^{\frac{1}{2}}$ appears, whence the residual estimator $\eta_{\text{R},D}$ is not robust in this case. Note also that as $-a \nabla p_h \cdot \mathbf{n}_\sigma = \mathbf{t}_h \cdot \mathbf{n}_\sigma$ for all $\sigma \subset \partial D$ in this case (cf. Section 5.3), one here actually comes to

$$\begin{aligned}
 \eta_{\text{DF},D} & \leq C \|p - p_h\|_D, \\
 \eta_{\text{R},D} & \leq \tilde{C} \|p - p_h\|_D,
 \end{aligned}$$

i.e., one has the local efficiency directly on each dual volume $D \in \mathcal{D}_h$ and not on the patch \mathcal{T}_{V_D} of the original simplicial elements sharing the vertex V_D .

Remark 6.7 (Local efficiency and robustness of the a posteriori error estimates for the finite element methods (3.6) and (3.8)). If a is piecewise constant on \mathcal{T}_h and under the other assumptions of Lemmas 3.8 and 3.11, we have by Corollary 3.12 that Remark 6.6 holds true also for the finite element method (3.6). On the other hand, when a is piecewise constant on \mathcal{D}_h , the finite element method with harmonic averaging (3.8) leads to a scheme which is very close to the harmonic-weighted vertex-centered finite volume method (3.5). Indeed, as $|D \cap K| = |K|/3$ for $D \in \mathcal{D}_h$

associated with one of the vertices of $K \in \mathcal{T}_h$ for the meshes of Section 2.1, the coefficient $\tilde{a}|_K$ from (3.7) is given by the harmonic averaging of the three values a_D , a_E , and a_F that a takes at the three dual volumes D , E , and F associated with the vertices of K . Consequently, for f piecewise constant on \mathcal{T}_h , (3.8) gives (3.5) where $\{\{a\}\}_\omega$ is now the harmonic average of a_D , a_E , and a_F . To obtain a guaranteed estimate, one defines $\mathbf{t}_h \in \mathbf{RTN}(\mathcal{S}_h)$ by fixing $\mathbf{t}_h \cdot \mathbf{n}$ on the boundary of $D \in \mathcal{D}_h^{\text{int}}$ by $-\tilde{a}\nabla p_h \cdot \mathbf{n}$ and by (5.12) for the other sides of \mathcal{S}_h , while separating the oscillations in f as in Theorem 5.7. Robustness can then be proved as in Theorem 6.1. In particular, there appears a sum over all $L \in \mathcal{S}_D; L \subset K$ in (6.3).

Remark 6.8 (Unconditioned dual norm robustness). Note that Theorem 6.4 gives full robustness with respect to the discontinuities in a without any restriction on a for any of the methods considered in the paper. In fact, tensor-valued \mathbf{A} can also be considered, cf. Remark 3.18. However, this result is established in the dual norm $\|\cdot\|_{\#}$ and one only has global efficiency.

7. NUMERICAL EXPERIMENTS

We present in this section the results of several numerical experiments.

7.1. A one-dimensional example with a smooth solution. We begin with a one-dimensional model problem

$$\begin{aligned} -p'' &= \pi^2 \sin(\pi x) && \text{in }]0, 1[, \\ p &= 0 && \text{in } 0, 1. \end{aligned}$$

The exact solution is smooth and given by $p(x) = \sin(\pi x)$. We consider the vertex-centered finite volume method (3.4) on a series of uniformly refined meshes and construct a one-dimensional equivalent of the equilibrated field \mathbf{t}_h given by (5.8). The results (we consider here the energy norm case of Theorem 5.1) are reported in Figure 2. It turns out that in this one-dimensional setting, one actually has $(\nabla \cdot \mathbf{t}_h, 1)_K = (f, 1)_K$ for all $K \in \mathcal{S}_h$ instead of (5.1) and hence the residual estimators $\eta_{R,D}$ represent a contribution of higher order and are only significant on coarsest meshes. Define the experimental order of convergence (e.o.c.) by

$$\text{e.o.c.} := \frac{\log(e_N) - \log(e_{N-1})}{\frac{1}{d} \log |\mathcal{V}_{N-1}| - \frac{1}{d} \log |\mathcal{V}_N|};$$

here e_N is the error on the last mesh, e_{N-1} is the error on the last but one mesh, and $|\mathcal{V}_N|$ and $|\mathcal{V}_{N-1}|$ denote the corresponding number of vertices. The e.o.c. is equal to 1.001 here.

7.2. Robust energy norm estimates for the vertex-centered finite volume method with harmonic averaging. We consider here a model problem taken from [32], where $\Omega = (-1, 1) \times (-1, 1)$ is divided into four subdomains Ω_i along the Cartesian axes (the subregion $\{x > 0, y > 0\} \cap \Omega$ is denoted by Ω_1 and the subsequent numbering is done counterclockwise) and a is constant and equal to a^i in Ω_i . Supposing in addition that $f = 0$, analytical solution writing

$$p(r, \theta) = r^\alpha (a_i \sin(\alpha\theta) + b_i \cos(\alpha\theta))$$

in each Ω_i can be found. Here (r, θ) are the polar coordinates in Ω , a_i and b_i are constants depending on Ω_i , and α is a parameter. This solution is continuous across the interfaces but only the normal component of its flux $\mathbf{u} = -\mathbf{S}\nabla p$ is continuous;

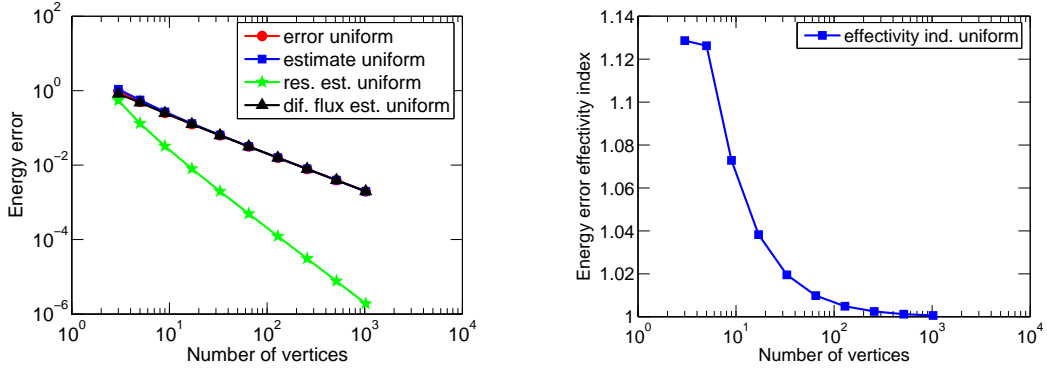


FIGURE 2. Estimated and actual energy error (left) and corresponding effectivity index (right) for the one-dimensional example

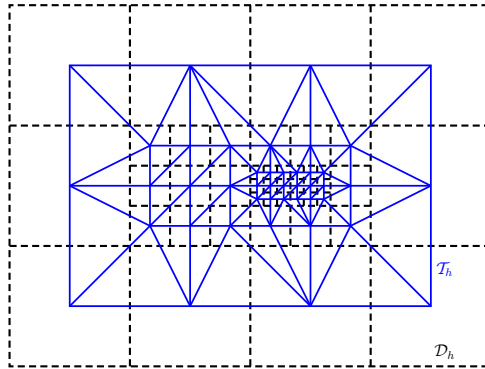


FIGURE 3. Example of a given nonmatching dual mesh \mathcal{D}_h and the corresponding primal triangular mesh \mathcal{T}_h for the harmonic-weighted vertex-centered finite volume method (3.5)

it exhibits a singularity at the origin and it only belongs to $H^{1+\alpha}(\Omega)$. We assume Dirichlet boundary conditions given by this solution and consider two sets of the coefficients. In the first one, $a^1 = a^3 = 5$, $a^2 = a^4 = 1$, $\alpha = 0.53544095$, and in the second one, $a^1 = a^3 = 100$, $a^2 = a^4 = 1$, $\alpha = 0.12690207$. The corresponding values of a_i , b_i can be found in [32, 41].

In order to get robust energy norm a posteriori error estimates, we know from Theorem 6.1 that a has to be piecewise constant on \mathcal{D}_h . If, however, we would first construct a simplicial mesh \mathcal{T}_h of Ω and then a dual grid \mathcal{D}_h as in Section 2.1, it would be very difficult to keep the dual mesh aligned with the inhomogeneities, especially for adaptive refinement. A possible solution is to first define the dual mesh \mathcal{D}_h and only then the primal one \mathcal{T}_h . On the resulting couple of grids \mathcal{D}_h , \mathcal{T}_h , we then use the weighted vertex-centered finite volume method (3.5). Recall that on square grids (and their uniform refinements), this method is equivalent to the weighted cell-centered finite volume one, cf. Corollary 3.14, as well as to the finite difference one, cf. Remark 3.17. The advantage of the scheme (3.5) is that it can be used also when the original square grid has been locally refined (into a nonmatching

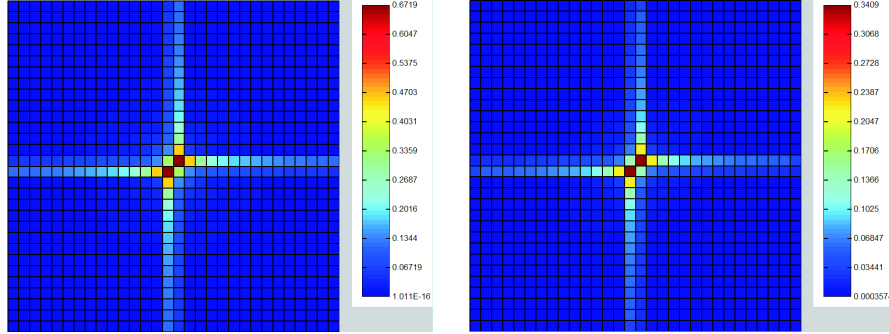


FIGURE 4. Estimated (left) and actual (right) energy error distribution on a uniformly refined mesh, $\alpha = 0.535$, harmonic-weighted vertex-centered finite volume method (3.5)

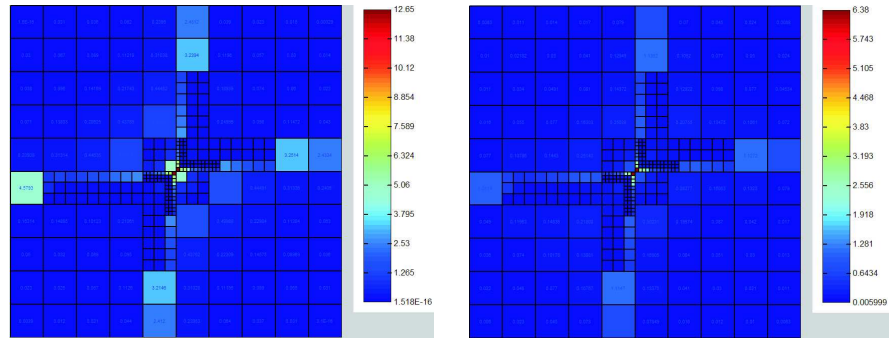


FIGURE 5. Estimated (left) and actual (right) energy error distribution on an adaptively refined mesh, $\alpha = 0.127$, harmonic-weighted vertex-centered finite volume method (3.5)

grid) as in Figure 3. Note however that the symmetry of this scheme is then lost. We remark that the present methodology works also for the finite element method with harmonic averaging (3.7), which stays symmetric.

We in Figure 4 present the predicted and actual distribution of the error for $\alpha = 0.535$ and uniform mesh refinement, using the estimators of Theorem 5.1 on the dual mesh \mathcal{D}_h and with \mathbf{t}_h given by (5.12) (the interpolation error on nonhomogeneous Dirichlet boundary conditions is neglected). A similar comparison, this time for adaptive mesh refinement and $\alpha = 0.127$, is shown in Figure 5. A square cell of the original dual mesh is refined into 9 identical subsquares if the estimated energy error is greater than 50% of the maximum of the estimators. We can see that in both cases the predicted error distribution is excellent and that in particular, the singularity at the origin is well detected. These results clearly illustrate the robust local lower bound of Theorem 6.1. We finally in Figure 6 give examples of the approximate solutions on the adaptively refined meshes in both cases; the strength of the singularity in the second case is quite obvious.

Knowing precisely the error distribution and refining adaptively the meshes, the next step is to check whether this leads to an increased efficiency of the calculations.

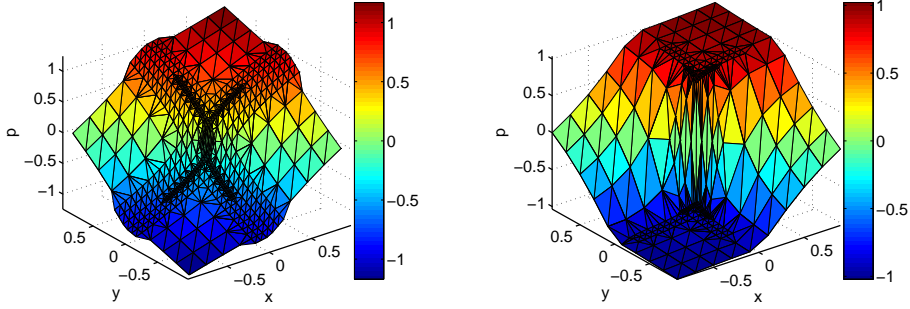


FIGURE 6. Approximate solutions on adaptively refined meshes, $\alpha = 0.535$ (left) and $\alpha = 0.127$ (right), harmonic-weighted vertex-centered finite volume method (3.5)

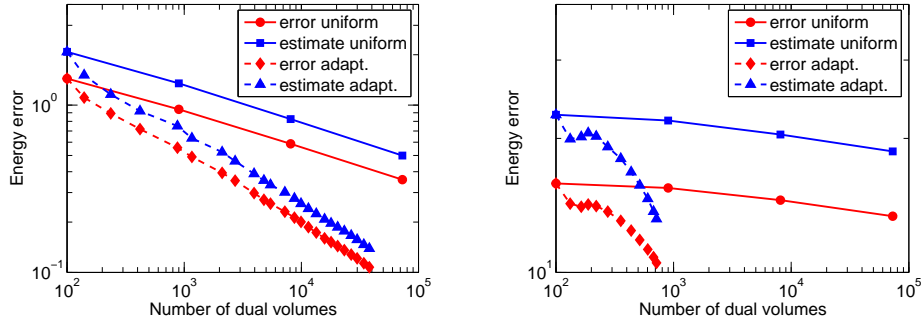


FIGURE 7. Estimated and actual energy errors for $\alpha = 0.535$ (left) and $\alpha = 0.127$ (right), harmonic-weighted vertex-centered finite volume method (3.5), estimates with local minimization (5.9)

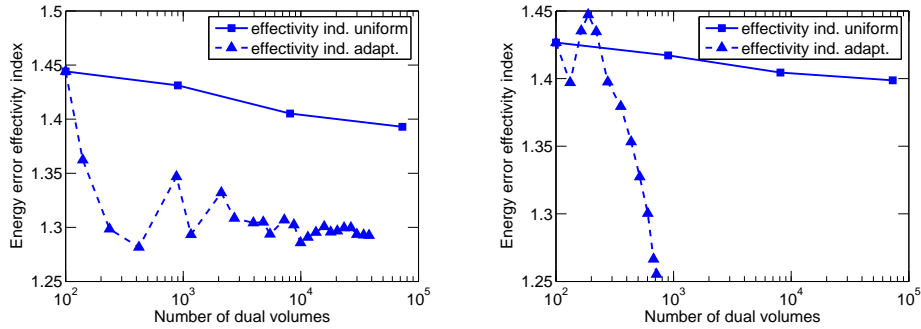


FIGURE 8. Energy error effectivity indices for $\alpha = 0.535$ (left) and $\alpha = 0.127$ (right), harmonic-weighted vertex-centered finite volume method (3.5), estimates with local minimization (5.9)

This is illustrated in Figure 7, from which it is evident that one can achieve a given precision with much fewer elements using adaptive mesh refinement based on our estimator. Here, the error in the energy norm (2.8) is approximated with a 7-point quadrature formula in each subtriangle $K \in \mathcal{S}_D$. In the code TALISMAN, which we use for numerical computations in this section, at most 9 levels of refinement can be used. This technical limitation is the reason why we in the adaptive case and for $\alpha = 0.127$ only present results with at most 716 dual volumes—this maximal refinement level is achieved near the origin but the maximal error is still located there. For $\alpha = 0.535$, the e.o.c. for uniform refinement was 0.449 and for the adaptive one 1.006. For $\alpha = 0.127$, these values were respectively 0.0757 and 1.024. Following [6], the somewhat slower convergence rate for uniform refinement (compare with the finite element case below) in the energy norm is related to the fact that the coefficient a is not aligned with the mesh \mathcal{T}_h .

Finally, in Figure 8, we give the effectivity indices using the local minimization approach described in Section 5.2.3. We can clearly observe a confirmation of the robustness of our estimators: whereas the inhomogeneity ratio rises from 5 to 100, the effectivity indices stay at the level of 1.4 for uniform refinement and improve for adaptive refinement. Moreover, the local minimization of Section 5.2.3 allows for almost asymptotic exactness, and this even in the case of discontinuous coefficients and singular solutions.

7.3. Energy estimates for the finite element method based on local Neumann/Dirichlet mixed finite element problems. For the same model problem as in the previous section, we present here the results for the finite element method (3.6) with the energy error estimators of Theorem 5.1 based on local Neumann/Dirichlet mixed finite element problems of Section 5.2.4 (thus $\mathcal{D}_h^{\text{int}} = \mathcal{S}_h$ and $\mathcal{D}_h^{\text{ext}} = \emptyset$ in Theorem 5.1). The initial mesh consisted of 24 right-angled triangles, conforming with the 4 subdomains (for the corresponding mesh \mathcal{S}_h , we refer to Figure 11).

Figure 9 shows the estimated and actual energy errors using the estimators based on the local Neumann/Dirichlet mixed finite element problems described in Section 5.2.4. For $\alpha = 0.535$, the e.o.c. for uniform refinement is 0.537 and for the adaptive one 0.999; for $\alpha = 0.127$, these values are, respectively, 0.172 and 0.946. This is fully in agreement with the smoothness of the weak solutions (recall that $p \in H^{1+\alpha}(\Omega)$) for the uniform refinement and shows optimal behavior of the adaptive refinement strategy. For $\alpha = 0.127$, the adaptive refinement is stopped for roughly 700 elements as the diameter of the smallest triangles near the origin reaches 10^{-16} which is the computer double precision.

The corresponding effectivity indices are presented in Figure 10. As predicted by the theory, we can observe in comparison with Figure 8 that the estimates are no more robust with respect to the discontinuities in a . The effectivity index is around 1.6 for $\alpha = 0.535$ and 4.7 for $\alpha = 0.127$, although it gets down to 1.27 for adaptive mesh refinement. As seen from Figure 11, the biggest overestimation appears in the central dual volume and the error distribution is no more predicted accurately (compare with Figures 4 and 5). The two forthcoming sections improve on these points.

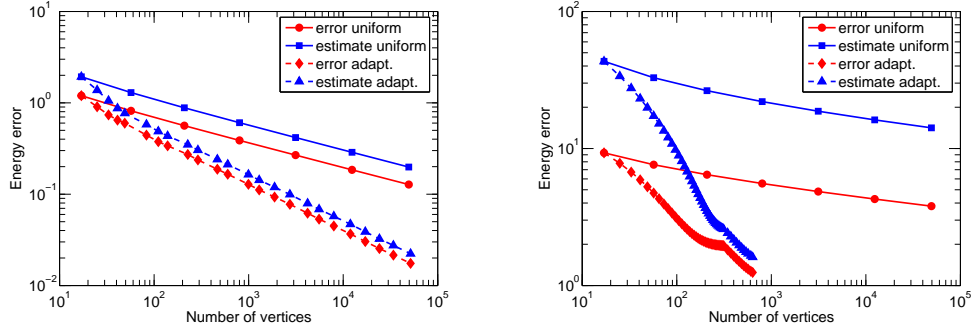


FIGURE 9. Estimated and actual energy errors for $\alpha = 0.535$ (left) and $\alpha = 0.127$ (right), finite element method (3.6), estimates by local Neumann/Dirichlet mixed finite element problems (5.10)

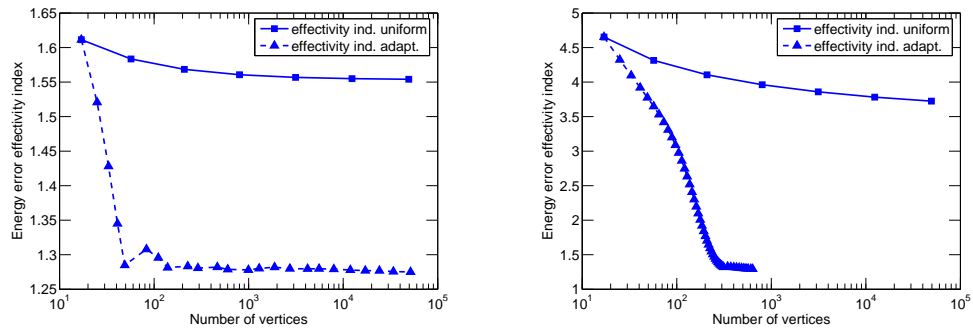


FIGURE 10. Energy error effectivity indices for $\alpha = 0.535$ (left) and $\alpha = 0.127$ (right), finite element method (3.6), estimates by local Neumann/Dirichlet mixed finite element problems (5.10)

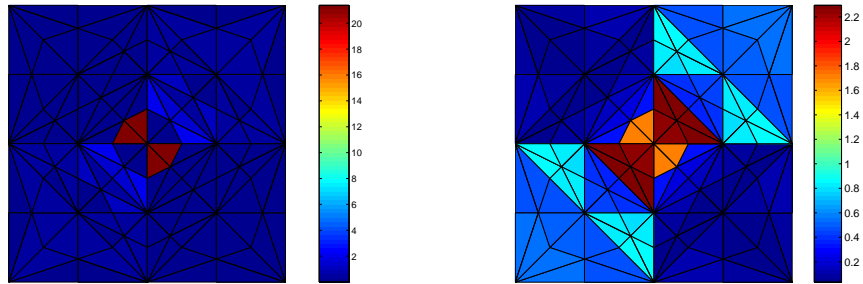


FIGURE 11. Estimated (left) and actual (right) energy error distribution on \mathcal{S}_h for $\alpha = 0.127$, finite element method (3.6), estimates by local Neumann/Dirichlet mixed finite element problems (5.10)

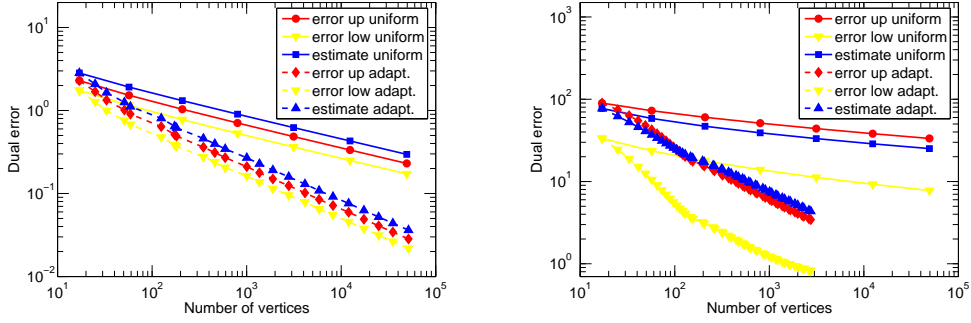


FIGURE 12. Estimated and actual dual errors for $\alpha = 0.535$ (left) and $\alpha = 0.127$ (right), finite element method (3.6), estimates by local Neumann/Dirichlet mixed finite element problems (5.10)

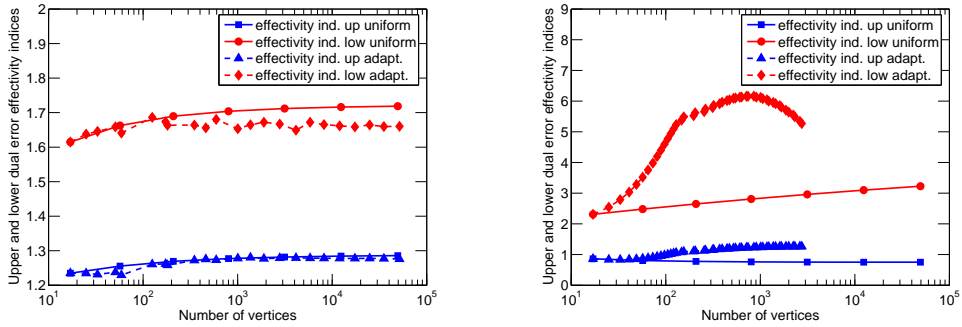


FIGURE 13. Dual error effectivity indices for $\alpha = 0.535$ (left) and $\alpha = 0.127$ (right), finite element method (3.6), estimates by local Neumann/Dirichlet mixed finite element problems (5.10)

7.4. Robust dual norm estimates for the finite element method. With the same setting as in the previous section, we now switch to the estimates in the dual norm (2.9) of Corollary 5.2. We still define \mathbf{t}_h by (5.10).

Figure 12 reports the estimated and actual dual error; here ‘error up’ means the computable upper bound on the dual error from (2.10), whereas ‘error down’ means the computable lower bound from (2.10). In the dual error upper bound, for $\alpha = 0.535$, the e.o.c. for uniform refinement is 0.539 and for the adaptive one 0.991; for $\alpha = 0.127$, these values are, respectively, 0.195 and 1.152. In Figure 13, we then report the corresponding effectivity indices. As predicted by Theorem 6.4, the estimates in the dual norm are fully robust. In particular, the effectivity index in the dual error upper bound is stable around the optimal value of 1; note that its values below 1 are possible since the estimates are derived for the dual norm and not for this upper bound. One conclusion from Figures 12 and 13 is that now the nonrobustness has been shifted to the gap between the computable upper and lower bounds for the dual error. Finally, Figure 14 shows the predicted dual error distribution and actual dual upper bound error distribution which reveals excellent (note in particular that there is no gap in the scales of the figures).

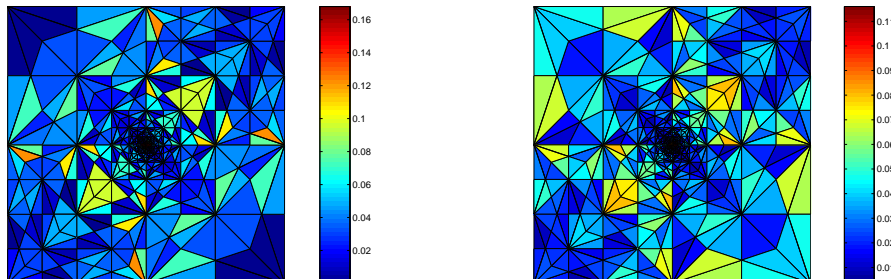


FIGURE 14. Estimated (left) and actual (right) dual error distribution on \mathcal{S}_h for $\alpha = 0.535$, finite element method (3.6), estimates by local Neumann/Dirichlet mixed finite element problems (5.10)

7.5. Energy norm estimates based on local refinements of individual dual volumes. We finally come back shortly to the energy norm framework of Section 7.3. The idea is to solve the mixed finite element minimization problem (5.10) on a local refinement of the mesh \mathcal{S}_D in individual dual volumes $D \in \mathcal{D}_h$, with the hope to decrease the error estimates in individual dual volumes. The local refinement is driven by the quantity $\|a^{\frac{1}{2}}\nabla p_h + a^{-\frac{1}{2}}\mathbf{t}_h\|_K$ on each element K of the local refinement of \mathcal{S}_D . We refine here only the central dual volume, as only in this dual volume the overestimation dependent on the jumps in a occurs. Figure 15 shows that this indeed enables to substantially decrease the effectivity indices (to be compared with Figure 10), although robustness is only achieved for $\alpha = 0.535$; for $\alpha = 0.127$, still an overestimation by a factor of 2.1 appears. Such a procedure also allows to predict much more precisely the error distribution, see the right part of Figure 16, in comparison with Figure 11. Another possible use of the independent refinement of only those dual volumes where the error indicator is large is to include the obtained local refinement to the mesh of the entire domain. Such a procure is illustrated in the left part of Figure 16, and, in the present case, allows to substantially improve the classical local refinement illustrated in the right part of Figure 10. Note that only two steps of the local refinement cycle on the global level allow to achieve the same precision as 49 steps in Section 7.3. Finally, the predicted and actual error distribution in the locally refined central dual volume is shown in Figure 17. It indicates that with the boundary conditions on ∂D given by $-\{a\nabla p_h \cdot \mathbf{n}_\sigma\}$, one cannot obtain a robust estimate and correct error distribution in the energy norm setting for the finite element method (3.6) even with such a local refinement of one dual volume; a larger domain would probably be necessary, indicating the nonlocality of the error distribution. Thus, in confirmation of the theory of Section 6, only the approaches of Sections 7.2 and 7.4 seem to give robust estimates (and correct error distribution).

REFERENCES

1. Mark Ainsworth, *Robust a posteriori error estimation for nonconforming finite element approximation*, SIAM J. Numer. Anal. **42** (2005), no. 6, 2320–2341. MR MR2139395
2. ———, *A synthesis of a posteriori error estimation techniques for conforming, non-conforming and discontinuous Galerkin finite element methods*, Recent advances in adaptive

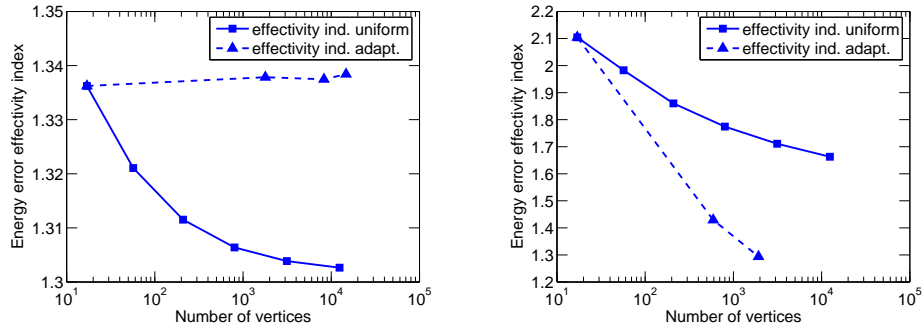


FIGURE 15. Energy error effectivity indices for $\alpha = 0.535$ (left) and $\alpha = 0.127$ (right), finite element method (3.6), estimates by local refinements of individual dual volumes

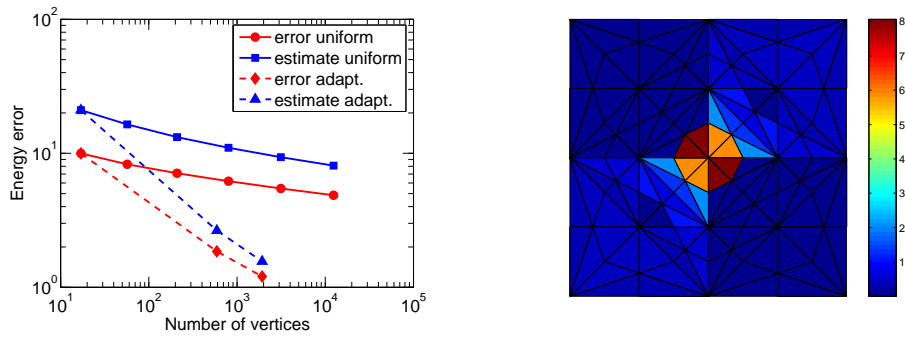


FIGURE 16. Estimated and actual energy error for $\alpha = 0.127$ (left) and estimated energy error distribution, finite element method (3.6), estimates by local refinements of ind. dual volumes

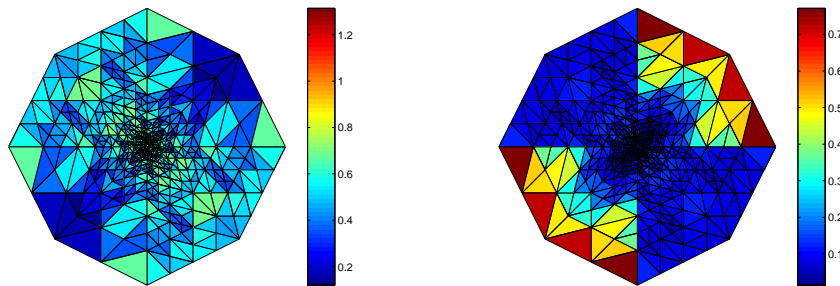


FIGURE 17. Estimated (left) and actual (right) energy error distribution on the locally refined central dual volume, $\alpha = 0.127$, finite element method (3.6)

- computation, Contemp. Math., vol. 383, Amer. Math. Soc., Providence, RI, 2005, pp. 1–14. MR MR2195792 (2006m:65234)
3. Mark Ainsworth and J. Tinsley Oden, *A posteriori error estimation in finite element analysis*, Pure and Applied Mathematics (New York), Wiley-Interscience [John Wiley & Sons], New York, 2000. MR MR1885308 (2003b:65001)
 4. D. N. Arnold and F. Brezzi, *Mixed and nonconforming finite element methods: implementation, postprocessing and error estimates*, RAIRO Modél. Math. Anal. Numér. **19** (1985), no. 1, 7–32. MR MR813687 (87g:65126)
 5. I. Babuška and W. C. Rheinboldt, *Error estimates for adaptive finite element computations*, SIAM J. Numer. Anal. **15** (1978), no. 4, 736–754. MR MR0483395 (58 #3400)
 6. Ivo Babuška, *personal communication*, 2008.
 7. Randolph E. Bank and Donald J. Rose, *Some error estimates for the box method*, SIAM J. Numer. Anal. **24** (1987), no. 4, 777–787. MR MR899703 (88j:65235)
 8. M. Bebendorf, *A note on the Poincaré inequality for convex domains*, Z. Anal. Anwendungen **22** (2003), no. 4, 751–756. MR MR2036927 (2004k:26025)
 9. C. Bernardi and R. Verfürth, *Adaptive finite element methods for elliptic equations with non-smooth coefficients*, Numer. Math. **85** (2000), no. 4, 579–608. MR MR1771781 (2001e:65177)
 10. Dietrich Braess and Joachim Schöberl, *Equilibrated residual error estimator for edge elements*, Math. Comp. **77** (2008), no. 262, 651–672. MR MR2373174
 11. Franco Brezzi and Michel Fortin, *Mixed and hybrid finite element methods*, Springer Series in Computational Mathematics, vol. 15, Springer-Verlag, New York, 1991. MR MR1115205 (92d:65187)
 12. C. Carstensen and S. A. Funken, *Constants in Clément-interpolation error and residual based a posteriori error estimates in finite element methods*, East-West J. Numer. Math. **8** (2000), no. 3, 153–175. MR MR1807259 (2002a:65173)
 13. Alexandra L. Chaillou and Manil Suri, *Computable error estimators for the approximation of nonlinear problems by linearized models*, Comput. Methods Appl. Mech. Engrg. **196** (2006), no. 1-3, 210–224. MR MR2270132 (2007g:65104)
 14. Ibrahim Cheddadi, Radek Fučík, Mariana I. Prieto, and Martin Vohralík, *Computable a posteriori error estimates in the finite element method based on its local conservativity: improvements using local minimization*, ESAIM Proc. **24** (2008), 77–96.
 15. ———, *Guaranteed and robust a posteriori error estimates for singularly perturbed reaction-diffusion problems*, *M2AN Math. Model. Numer. Anal.*, to appear, 2009.
 16. Zhiming Chen and Shubin Dai, *On the efficiency of adaptive finite element methods for elliptic problems with discontinuous coefficients*, SIAM J. Sci. Comput. **24** (2002), no. 2, 443–462. MR MR1951050 (2003k:65160)
 17. Philippe Destuynder and Brigitte Métivet, *Explicit error bounds in a conforming finite element method*, Math. Comp. **68** (1999), no. 228, 1379–1396. MR MR1648383 (99m:65211)
 18. Alexandre Ern, Annette F. Stephansen, and Martin Vohralík, *Improved energy norm a posteriori error estimation based on flux reconstruction for discontinuous Galerkin methods*, Preprint R07050, Laboratoire Jacques-Louis Lions & HAL Preprint 00193540 version 1 (14-11-2007), Université Paris 6 and Ecole des Ponts, 2007.
 19. Alexandre Ern and Martin Vohralík, *Flux reconstruction and a posteriori error estimation for discontinuous Galerkin methods on general nonmatching grids*, C. R. Math. Acad. Sci. Paris **347** (2009), 441–444.
 20. Robert Eymard, Thierry Gallouët, and Raphaële Herbin, *Finite volume methods*, Handbook of Numerical Analysis, Vol. VII, North-Holland, Amsterdam, 2000, pp. 713–1020. MR MR1804748 (2002e:65138)
 21. Francesca Fierro and Andreas Veiser, *A posteriori error estimators, gradient recovery by averaging, and superconvergence*, Numer. Math. **103** (2006), no. 2, 267–298. MR MR2222811 (2007a:65178)
 22. Sergey Korotov, *Two-sided a posteriori error estimates for linear elliptic problems with mixed boundary conditions*, Appl. Math. **52** (2007), no. 3, 235–249. MR MR2316154
 23. P. Ladevèze, *Comparaison de modèles de milieux continus*, Ph.D. thesis, Université Pierre et Marie Curie (Paris 6), 1975.
 24. P. Ladevèze and D. Leguillon, *Error estimate procedure in the finite element method and applications*, SIAM J. Numer. Anal. **20** (1983), no. 3, 485–509. MR MR701093 (84g:65150)

25. Frank W. Letniowski, *Three-dimensional Delaunay triangulations for finite element approximations to a second-order diffusion operator*, SIAM J. Sci. Statist. Comput. **13** (1992), no. 3, 765–770. MR MR1157598 (93a:65153)
26. R. Luce and B. I. Wohlmuth, *A local a posteriori error estimator based on equilibrated fluxes*, SIAM J. Numer. Anal. **42** (2004), no. 4, 1394–1414. MR MR2114283 (2006d:65122)
27. L. E. Payne and H. F. Weinberger, *An optimal Poincaré inequality for convex domains*, Arch. Rational Mech. Anal. **5** (1960), 286–292. MR MR0117419 (22 #8198)
28. Martin Petzoldt, *A posteriori error estimators for elliptic equations with discontinuous coefficients*, Adv. Comput. Math. **16** (2002), no. 1, 47–75. MR MR1888219 (2002m:65110)
29. W. Prager and J. L. Synge, *Approximations in elasticity based on the concept of function space*, Quart. Appl. Math. **5** (1947), 241–269. MR MR0025902 (10,81b)
30. Mario Putti and Christian Cordes, *Finite element approximation of the diffusion operator on tetrahedra*, SIAM J. Sci. Comput. **19** (1998), no. 4, 1154–1168. MR MR1614315 (99d:65325)
31. S. I. Repin, *A posteriori error estimation for nonlinear variational problems by duality theory*, Zap. Nauchn. Sem. S.-Peterburg. Otdel. Mat. Inst. Steklov. (POMI) **243** (1997), no. Kraev. Zadachi Mat. Fiz. i Smezh. Vopr. Teor. Funktsii. 28, 201–214, 342. MR MR1629741 (99e:49049)
32. Béatrice Rivière, Mary Fanett Wheeler, and K. Banas, *Part II. Discontinuous Galerkin method applied to single phase flow in porous media*, Comput. Geosci. **4** (2000), no. 4, 337–349.
33. Jean E. Roberts and J.-M. Thomas, *Mixed and hybrid methods*, Handbook of Numerical Analysis, Vol. II, North-Holland, Amsterdam, 1991, pp. 523–639. MR MR1115239
34. Joachim Schöberl, *personal communication*, 2009.
35. T. Strouboulis, I. Babuška, and S. K. Gangaraj, *Guaranteed computable bounds for the exact error in the finite element solution. II. Bounds for the energy norm of the error in two dimensions*, Internat. J. Numer. Methods Engrg. **47** (2000), no. 1-3, 427–475, Richard H. Gallagher Memorial Issue. MR MR1744296 (2001a:65109)
36. J. L. Synge, *The hypercircle in mathematical physics: a method for the approximate solution of boundary value problems*, Cambridge University Press, New York, 1957. MR MR0097605 (20 #4073)
37. Tomáš Vejchodský, *Guaranteed and locally computable a posteriori error estimate*, IMA J. Numer. Anal. **26** (2006), no. 3, 525–540. MR MR2241313
38. R. Verfürth, *A review of a posteriori error estimation and adaptive mesh-refinement techniques*, Teubner-Wiley, Stuttgart, 1996.
39. ———, *Robust a posteriori error estimates for stationary convection-diffusion equations*, SIAM J. Numer. Anal. **43** (2005), no. 4, 1766–1782. MR MR2182149
40. Martin Vohralík, *On the discrete Poincaré–Friedrichs inequalities for nonconforming approximations of the Sobolev space H^1* , Numer. Funct. Anal. Optim. **26** (2005), no. 7–8, 925–952. MR MR2192029
41. ———, *A posteriori error estimates for lowest-order mixed finite element discretizations of convection-diffusion-reaction equations*, SIAM J. Numer. Anal. **45** (2007), no. 4, 1570–1599. MR MR2338400
42. ———, *A posteriori error estimation in the conforming finite element method based on its local conservativity and using local minimization*, C. R. Math. Acad. Sci. Paris **346** (2008), no. 11-12, 687–690. MR MR2423279
43. ———, *Residual flux-based a posteriori error estimates for finite volume and related locally conservative methods*, Numer. Math. **111** (2008), no. 1, 121–158. MR MR2448206
44. ———, *Two types of guaranteed (and robust) a posteriori estimates for finite volume methods*, Finite Volumes for Complex Applications V, ISTE and John Wiley & Sons, London, UK and Hoboken, USA, 2008, pp. 649–656.
45. Jinchao Xu, Yunrong Zhu, and Qingsong Zou, *New adaptive finite volume methods and convergence analysis*, Preprint AM296, Mathematics Department, Penn State, 2006.
46. O. C. Zienkiewicz and J. Z. Zhu, *A simple error estimator and adaptive procedure for practical engineering analysis*, Internat. J. Numer. Methods Engrg. **24** (1987), no. 2, 337–357. MR MR875306 (87m:73055)

UPMC UNIV. PARIS 06, UMR 7598, LABORATOIRE JACQUES-LOUIS LIONS, 75005, PARIS, FRANCE

CNRS, UMR 7598, LABORATOIRE JACQUES-LOUIS LIONS, 75005, PARIS, FRANCE
E-mail address: vohralik@ann.jussieu.fr